SATBAYEV UNIVERSITY

Engineering Journal of Satbayev University

Volume 148 (2026), Issue 5, 8-26

https://doi.org/10.51301/ejsu.2026.i5.02

TiZrNbTa-based bio-high entropy alloys for biomedical applications: a comprehensive review

K.N.R. Shaik, A. Zhumabekova, A. Perveen*

School of Engineering, Nazarbayev University, Astana, Kazakhstan

**Corresponding author: asma.perveen@nu.edu.kz*

Abstract. The increasing demand for advanced biomedical implants has driven the development of novel metallic biomaterials with improved mechanical compatibility, corrosion resistance, and biocompatibility. Conventional implant materials such as Ti–6Al–4V, Co–Cr–Mo alloys, and stainless steel, often suffer from limitations including stress shielding, ion release, and long-term biological concerns. Among emerging biomaterials, TiZrNbTa-based bio-high entropy alloys (Bio-HEAs) have emerged as promising candidates due to their composition of biocompatible elements and their unique combination of high strength, low elastic modulus, excellent corrosion resistance, and favorable biocompatibility. This review summarizes recent developments in TiZrNbTa-based Bio-HEAs, with particular emphasis on microstructural evaluation, new elemental addition strategies, mechanical properties, corrosion behaviour, and biocompatibility. Reported studies demonstrated that TiZrNbTa-based Bio-HEAs exhibit stable body-centered cubic (BCC) solid-solution structures, although phase stability and microstructural characteristics can be tailored through compositional modifications, thermomechanical treatments, and advanced manufacturing processes. Depending on composition and processing conditions, TiZrNbTa-based Bio-HEAs exhibits the elastic modulus ranging from 57 to 135 GPa and yield strengths exceeding 1000 MPa providing a favorable balance between mechanical strength and compatibility with human bone. Furthermore, the formation of stable passive oxide films rich in TiO_2, ZrO_2, Nb_2O_5, and Ta_2O_5 contributes to excellent corrosion resistance in physiological environments. Biocompatibility studies have demonstrated favorable biological responses, highlighting the potential of TiZrNbTa-based Bio-HEAs for orthopedic and dental implant applications. Finally, current challenges and future research directions for the development of next-generation biomedical implants are discussed.

Keywords: *bio high entropy alloys, TiZrNbTa, microstructure, mechanical properties, biocompatibility, alloy elements*.

Received: 8 July 2026
Received in revised form: 12 October 2026
Accepted: 16 October 2026
Available online: 31 October 2026

1. Introduction

The increasing global population and rising prevalence of various musculoskeletal disorders have significantly increased the demand for advanced biomedical implants. Metallic biomaterials have become increasingly important in orthopedic and dental applications because of their superior properties including high load bearing capacity, fatigue resistance, and structural reliability. In addition to mechanical strength, implant materials must exhibit an excellent combination of high strength, corrosion resistance, and long-term biocompatibility to ensure safe and durable performance in complex physiological environments [1-2].

Conventional implant materials such as Co-Cr-Mo alloy, stainless steel and Titanium (Ti) alloys are widely used in clinical practice [3]. Although these materials have achieved considerable clinical success, they often fail to satisfy long-term functional recovery requirements and may require revision surgeries because of material related complications [4]. Ti alloys exhibit excellent biocompatibility and high strength; however, their relatively poor wear resistance can lead to the generation of metallic wear particles during long term service, potentially causing damage to the surrounding tissues [5-6]. Furthermore, 304 stainless steel is considered as one of the earliest metallic materials used for artificial joint implants. However, its high elastic modulus compared with that of human bone reduces effective load transfer between the implant and surrounding tissue, resulting in stress shielding. This phenomenon can lead to bone resorption, degradation of surrounding bone tissue, and eventual implant failure during long-term service [7, 8, 9]. In addition, conventional alloys may contain potentially cytotoxic elements such as Aluminum (Al) and Vanadium (V), which have been associated with neurological disorders and inflammatory reactions. The elastic modulus of Ti alloys is 120 GPa and stainless steel is 193 GPa significantly higher than that of human bone of 10-35 GPa [10]. As a result, developing biomaterials with enhanced mechanical compatibility and biological safety has become a major objective in modern biomedical engineering.

To address these challenges, high-entropy alloys (HEAs) have emerged as a new class of advanced materials that challenge conventional alloy design principles. HEAs consist of multiple principal elements and are stabilized by high configurational entropy which promotes the formation of simple

© 2026. K.N.R. Shaik, A. Zhumabekova, A. Perveen
rasool.shaik@nu.edu.kz; anel.zhumabekova@nu.edu.kz; asma.perveen@nu.edu.kz
Engineering Journal of Satbayev University. eISSN 2959-2348. Published by Satbayev University
This is an Open Access article distributed under the terms of the Creative Commons Attribution License (http://creativecommons.org/licenses/by/4.0/), which permits unrestricted reuse, distribution, and reproduction in any medium, provided the original work is properly cited.

solid-solution phases [11, 12, 13]. HEAs exhibits four core effects, namely high entropy effect, severe lattice distortion effect, sluggish diffusion effect, and cocktail effect. Together, these effects contribute to enhanced mechanical strength, corrosion resistance, and wear performance [14-16]. Furthermore, HEAs offer compositional flexibility, allowing properties to be tailored, including elastic modulus and improved biocompatibility, which are crucial for biomedical applications [16]. The term «Bio-HEA» was first introduced in 2019 to describe multi-principal-element alloys specifically designed for biomedical purposes [17, 18]. Since then, significant efforts have been devoted to developing Bio-HEAs with improved mechanical performance, corrosion resistance, and biological compatibility.

Among the diverse families of the HEAs, TiZrNbTa-based Bio-HEAs are considered as promising alloy for next-generation biomedical implants. This alloy system is composed entirely of biocompatible metallic elements with high biosafety and minimal allergenic potential. Several processing routes including Vacuum Arc Melting (VAM), Powder Metallurgy (PM) and Additive Manufacturing techniques (AM), have been widely used to fabricate these alloys. Because TiZrNbTa Bio-HEAs contain only non-toxic and biocompatible elements, they are considered highly suitable for biomedical applications.

Each constituent element in these alloys plays a distinct role in determining the overall properties of the alloy. Niobium (Nb) and Tantalum (Ta) act as strong β-phase stabilizers and improve corrosion resistance. Titanium (Ti) and Zirconium (Zr) contribute to excellent biocompatibility and the formation of stable passive oxide films. As a result, TiZrNbTa-based alloys typically exhibit relatively low elastic modulus values that are closer to the human bone than those of conventional implant materials. Furthermore, the formation of multicomponent oxide layers enhances corrosion resistance and reduces metallic ion release in physiological environments.

One of the major advantages of TiZrNbTa based Bio-HEAs is the ability to tailor their properties through compositional modification and alloying element additions. Strategic alloying additions can improve the balance of strength, ductility, corrosion resistance, and biological performance. Consequently, understanding the relationships between alloy composition, microstructure, phase evaluation, and resultant properties is essential for the rational design of biomedical HEAs. Although substantial progress has been achieved in the development of TiZrNbTa-based Bio-HEAs, several critical issues remain unresolved. The effect of alloying additions on phase stability, microstructural evaluation, mechanical properties, corrosion resistance, and biocompatibility has not yet been systematically reviewed. Common alloying elements investigated in this system include titanium (Ti), molybdenum (Mo), magnesium (Mg), zinc (Zn), cobalt (Co), zirconium (Zr), hafnium (Hf), tantalum (Ta), tungsten (W), silver (Ag), aluminum (Al), and tin (Sn) [19, 20]. Many of these elements have shown favorable biological compatibility and present opportunities for further property optimization.

The increasing prevalence of bone and joint disorders continues to drive the demand for implant materials with superior mechanical compatibility, corrosion resistance, and biocompatibility [21, 22]. Implant materials must simultaneously satisfy multiple, and often conflicting requirements, including high strength, low elastic modulus, resistance to corrosion and wear, and favorable biological responses. Achieving this combination of properties with conventional single-principal-element alloys remains challenging. In contrast, the exceptional compositional flexibility of HEAs offers new opportunities to develop multifunctional biomaterials capable of meeting these demanding requirements. Despite the growing number of studies on TiZrNbTa-based Bio-HEAs, a comprehensive understanding of how alloying additions influence microstructural evaluation, mechanical properties, corrosion behavior, and biocompatibility remains limited. Therefore, a critical and comprehensive review is necessary to summarize recent advancements and identify future research directions for the development of next-generation biomedical HEA.

This review provides a comprehensive assessment of TiZrNbTa-based Bio-HEAs, focusing on microstructural evaluation, alloying strategies, mechanical properties, corrosion behavior, and biocompatibility. Particular attention is given to the effects of compositional modifications on phase formation, microstructure stability and property optimization. Finally, current challenges and future research opportunities are discussed to support the development of advanced biomedical implant materials based on TiZrNbTa-derived Bio-HEAs.

2. Materials and methods

This review applies a comprehensive thematic and comparative approach to evaluate the current state of research on TiZrNbTa-based bio-high entropy alloys intended for biomedical applications. The reviewed studies were organized according to the main factors governing the structure and performance of these alloys, including chemical composition, alloying additions, processing routes, microstructural characteristics, mechanical properties, corrosion behavior, and biocompatibility. Particular attention was given to the relationships between compositional modification, phase constitution, microstructural evolution, and the resulting functional properties of TiZrNbTa-based Bio-HEAs.

The available experimental data were comparatively analyzed according to the principal characteristics reported in the literature. Microstructural assessment considered the formation and stability of BCC, dual-BCC, HCP, and other secondary phases, as well as elemental segregation, grain refinement, and microstructural changes induced by alloying and processing conditions. Mechanical performance was evaluated primarily in terms of Young's modulus, yield strength, hardness, ductility, and the balance between strength and elastic compatibility with human bone. Where appropriate, the properties of TiZrNbTa-based alloys were compared with those of conventional biomedical materials, including Ti–6Al–4V, Co–Cr–Mo alloys, and stainless steels.

Corrosion behavior was assessed using the electrochemical characteristics reported for different physiological and simulated environments, with particular consideration of corrosion potential, corrosion current density, passivation behavior, polarization resistance, impedance response, and the formation of protective oxide films. Biological performance was evaluated on the basis of the reported cytocompatibility, cell adhesion, viability and proliferation, surface wettability, and osteogenic responses, while also considering the influence of manufacturing and surface-modification methods. The collected evidence was synthesized to identify consistent trends, composition–processing–structure–property relationships, existing limitations, and promising directions for the further development of TiZrNbTa-based Bio-HEAs for biomedical implants.

3. Evaluation of TiZrNbTa-Based Bio-HEAs

3.1. Microstructure

The microstructural characteristics of TiZrNbTa based Bio HEAs plays a critical role in determining their mechanical properties, corrosion resistance, and long-term performance in biomedical environments. Owing to the high configurational entropy and similar atomic radius of the constituent refractory elements, these alloys generally form stable body-centered cubic (BCC) solid-solution structures. However, phase separation, elemental segregation, and secondary phase formation may occur depending on alloy composition, processing route, and heat-treatment conditions. Therefore, understanding the microstructural evaluation of TiZrNbTa-based Bio-HEAs is essential for optimizing their performance in biomedical applications.

Equiatomic TiZrNbTa alloys generally exhibit BCC solid solution structures with varying degrees of elemental segregation. Aranda et al. [23] investigated $Ti_{25}Nb_{25}Zr_{25}Ta_{25}$ alloy and reported a dual phase microstructure consisting of dendritic BCC1 and interdendritic BCC2 regions. The BCC1 phase exhibited a near equiatomic composition and remained chemically homogeneous, whereas the BCC2 phase was enriched in Ti and Zr and depleted in Nb and Ta. These observations indicate elemental partitioning during solidification without the formation of intermetallic compounds. Similarly, compositionally graded $Ti_{25}Zr_{50-x}Nb_xTa_{25}$ alloy fabricated by laser metal deposition (LMD) process and exhibited predominantly single-phase BCC structure for compositions ranging from $Ti_{25}Zr_0Nb_{50}Ta_{25}$ and $Ti_{25}Zr_{25}Nb_{25}Ta_{25}$. These alloys showed coarse dendritic microstructure, confirming stable solid-solution formation. As Zr/Nb ratio increases, finer microstructures developed together with the formation of a second BCC phase along grain boundaries [24].

Xiang et al. [25] investigated the microstructural evaluation of $Ti_{25}Zr_{25}Nb_{25}Ta_{25}$ alloy in both as-cast alloy and annealed conditions. The as-cast alloys exhibited a dual BCC phase microstructure consisting of fine equiaxed dendrites with compositional segregation between dendritic and interdendritic regions. Annealing at 400 to 600°C preserved the BCC microstructure while increasing the volume fraction of the BCC1 phase and promoting dendrite coarsening. At higher annealing temperatures 700-800°C, vein like grain boundary phase and spinodal decomposition structures were observed. These microstructural changes indicate thermally driven phase redistribution without the formation of intermetallic compounds. The influence of Ta content on microstructural evaluation was systematically investigated in arc-melted $Ti_{45}Zr_{45}Nb_5Ta_5$, $Ti_{42.5}Zr_{42.5}Nb_5Ta_{10}$, and $Ti_{40}Zr_{40}Nb_5Ta_{15}$ alloys. All compositions exhibit a single-phase BCC structure. Increasing Ta content reduced the lattice parameter from 3.434 Å to 3.419 Å, indicating lattice contraction associated with solid-solution strengthening. Furthermore, the average grain size decreased from 84.7 μm to 50.4 μm, demonstrating progressive grain refinement. Elemental maps revealed preferential segregation of Ta into dendritic regions, whereas Zr and Nb were enriched in interdendritic. This compositional partitioning is attributed to differences in melting temperatures and mixing enthalpy among the constituent elements [27].

The microstructural evaluation of equiatomic TiZrNbTa alloy was investigated by Liu et al. [31] in both the as cast and homogenized conditions. The as cast alloy exhibited a dual BCC microstructure containing of Nb and Ta-rich dendritic regions and Ti- and Zr-rich interdendritic regions. This indicating the elemental segregation during solidification. As shown in (Figure 1), Nb and Ta is partitioned into the dendritic region, while Ti and Zr were enriched in the interdendritic regions. After homogenization at 1100°C for 24 hours, the dendritic segregation was significantly reduced, resulting in a homogeneous BCC matrix, as shown in (Figure 2).

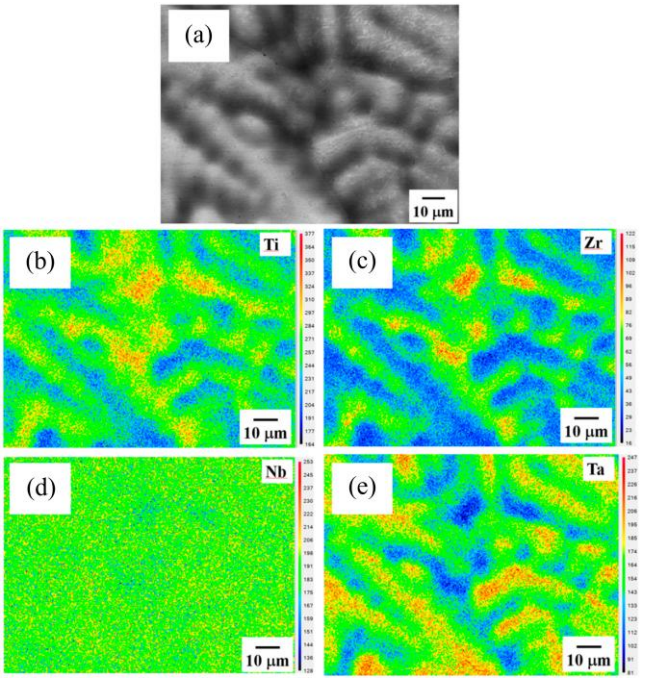


Figure 1. Scanning electron microscope (SEM) back-scatter image (BEI) of the as-cast $Ti_{25}Zr_{25}Nb_{25}Ta_{25}$ alloy shows composition mapping for Ti, Zr, Nb, and Ta. The Nb mapping does not clearly reveal the dendrites and inter-dendrites, likely due to the higher Lα X-ray energy of Nb (~2.169 eV) compared to Ta (~1.804 eV), which results in significant absorption in dendrite regions and an underestimated amount of Nb [31]

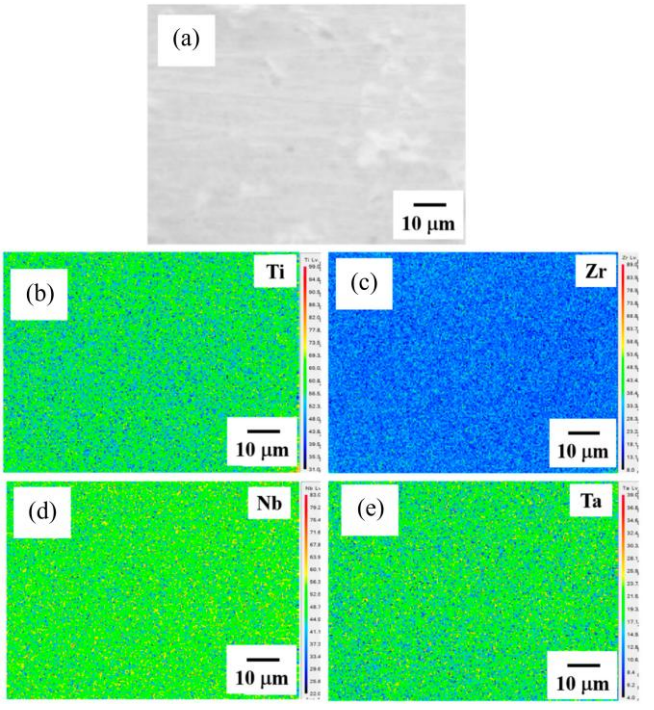


Figure 2. The SEM BEI of the as-homogenized $Ti_{25}Zr_{25}Nb_{25}Ta_{25}$ alloy, and the composition mapping for (b) Ti, (c) Zr, (d) Nb, and (e) Ta [31]

Furthermore, transmission electron microscopy (TEM) characterization revealed that the homogenized alloy presented a nanoscale spinodal decomposition, interconnected TiZr-rich and NbTa-rich BCC domains together with uniformly distributed α and ω nanoprecipitates. These findings demonstrate that the homogenization treatment effectively refined the microstructure while maintaining the overall BCC crystal structure. The influence of different process control agents (PCAs) such as stearic acid as solid PCA, ethanol, and n-heptane (liquid PCAs) on $Ti_{25}Zr_{25}Nb_{25}Ta_{25}$ alloy powders was investigated using mechanical alloying. During the milling process, the powder gradually transformed from a mixed HCP+BCC structure to a single BCC phase after 50 to 65 h of milling, indicating progressive interdiffusion among constituent elements. Extended milling reduced particle size to approximately 100 nm and increased lattice strain. Liquid PCAs, including ethanol and n-heptane, improved particle refinement and elemental homogenization by suppressing excessive cold welding [28]. Gonzalez-Guillén et al. [29] reported that equiatomic TiNbZrTa alloy fabricated via powder metallurgy exhibited a multiphase microstructure composed of BCC and FCC phases. The FCC phase occupied approximately 25-32 vol.% of the microstructure and was uniformly distributed within the BCC matrix. The presence of ZrC precipitates and refined grains indicates that powder metallurgy processing can significantly influence phase formation and microstructural refinement. These results highlight the important role of the processing route in controlling phase constitution and grain morphology in TiZrNbTa-based alloys.

Lu et al. [30] investigated a series of arc-melted alloys including $Nb(HfTa)_{0.4}TiZr$, $Nb(HfTa)_{0.25}TiZr$, $Nb(HfTa)_{0.17}TiZr$, $Nb(HfTa)_{0.1}TiZr$, and NbTiZr alloys. All alloys exhibited a single-phase BCC structure with uniform elemental distribution, and no secondary phases were observed in the cast condition. During mechanical deformation, localized stress-induced BCC-to-HCP phase transformation occurred. Furthermore, decreasing Hf/Ta ratio reduced the amount of transformed HCP structures and increased structural disorder, indicating a strong compositional dependence of phase stability.

The studies discussed above demonstrated that alloy composition and processing conditions strongly influence phase constitution and microstructural stability in TiZrNbTa-based Bio HEAs. Most reported alloys exhibit stable BCC solid-solution structures. However, variations in composition, thermal treatment, and manufacturing route can promote dual-BCC structures, spinodal decomposition, grain refinement, and deformation-induced phase transformations. In general, phase stability is governed by lattice distortion, valence electron concentration, and thermodynamic mixing behavior. These microstructural characteristics directly influence the mechanical properties, corrosion resistance, and elastic modulus of the alloys. Therefore, understanding the relationship between composition, processing conditions, and microstructural evaluation is essential for the rational design of next-generation TiZrNbTa-based Bio HEAs. Table 1 summarizes the compositions, processing methods, conditions, and resulting microstructural phases of the reported alloys.

3.2. Mechanical properties

Biomedical implants serve as substitutes for damaged bones or provide structural support in orthopedic and dental applications. Therefore, the mechanical compatibility between the implant material and surrounding biological tissues plays a critical role in determining clinical performance and long-term success [7]. A suitable balance between strength, stiffness, and ductility is required to ensure stable load transfer and long-term functionality under physiological conditions [43]. An elastic modulus that is too low may compromise structural support, whereas an excessively high modulus can lead to stress shielding, thereby impairing bone remodeling and reducing implant longevity.

One of the major limitations of conventional biomaterials, such as Ti–6Al–4V and Co–Cr–Mo alloys, is the significant mismatch between their elastic modulus and that of human cortical bone (10 to 30 GPa) [44, 45]. As summarized in Table 2, these materials possess substantially higher stiffness than bone tissue. Consequently, the implant bears a disproportionate share of the applied load, leading to stress shielding, bone resorption, reduced bone density, and eventual implant failure. Therefore, modern biomaterial design emphasizes mechanical compatibility with biological tissues rather than maximizing strength alone [27, 46].

TiZrNbTa-based Bio HEAs have emerged as promising candidates for next-generation biomedical implants because they combine high strength with a relatively low elastic modulus and offer excellent corrosion resistance and biocompatibility [25, 51]. The mechanical performance of these alloys is strongly influenced by multi-principal-element composition and microstructural stability. Key strengthening mechanisms include solid solution strengthening, lattice distortion, and phase stability within the BCC structure [52, 53]. Together, these characteristics contribute to improved load transfer, reduced stress shielding, and enhanced long term reliability for biomedical applications [54].

In the TiZrNbTa-based Bio HEA system, Niobium (Nb) plays a critical role as a strengthening element because of its relatively large atomic radius, which promotes severe lattice distortion and solid-solution strengthening. The addition of Nb enhances yield strength and hardness while maintaining phase stability within the BCC structure [55]. Furthermore, Ti also contributes to solid-solution strengthening but its effectiveness depends strongly on concentration [56]. At relatively lower concentration, Ti promotes the formation of a stable BCC solid solution and improves mechanical performance. In contrast, excessive Ti addition may promote intermetallic phase formation, resulting in reduced ductility and increased brittleness [14].

The mechanical properties of TiZrNbTa alloys are highly composition dependent. Increasing the concentration of Ti and Zr generally reduces young's modulus, thereby improving mechanical compatibility with bone tissue, although this may be accompanied by a reduction in yield strength. Conversely, increasing the Nb and Ta content enhances lattice distortion and stronger atomic bonding strength within the BCC structure, resulting in improved strength and hardness [57]. Li et al. [27] systematically investigated the effect of Ta content on the mechanical properties of $Ti_{45}Zr_{45}Nb_5Ta_5$, $Ti_{42.5}Zr_{42.5}Nb_5Ta_{10}$, and $Ti_{40}Zr_{40}Nb_5Ta_{15}$ alloys. Increasing the Ta content from 5 to 15 at% increased the yield strength from approximately 626.7 MPa to 990 MPa, while the elastic modulus increased from 59.3 to 73.1 GPa. Despite this strengthening effect, tensile ductility remained relatively stable at 18.8 to 20%. In addition, hardness values increased from 220 HV to 324 HV with increasing Ta content. These results demonstrated that Ta addition is an effective strategy for enhancing strength while maintaining acceptable mechanical compatibility for biomedical applications.

Table 1. Summary of processing routes, processing conditions, and microstructural for TiZrNbTa BIO HEAs

Methods	Alloy	Condition	Microstructural phase	References
VAC	TiNbTaZr	As cast	BCC1+BCC2	[32]
VAC+ Suction casting	$Ti_{25}Zr_{25}Nb_{25}Ta_{25}$	As cast	BCC	[33]
VAC + vacuum annealing	$Ti_{25}Zr_{25}Nb_{25}Ta_{25}$	Annealed 1123 K, 1 h	BCC	[33]
Arc melting	TiNbTaZr	As cast	BCC	[34]
Arc melting	TiNbTaZr	Annealed 500-900°C, 100 h	BCC1 + BCC2	
Arc melting	TiNbTaZr	Annealed 1000-1100°C, 100 h	BCC1 + BCC2 + BCC3	
Arc melting	TiNbTaZr	Annealed 1200=1300°C, 100 h	BCC + HCP	
VAC	$Ti_{40}Zr_{25}Nb_{25}Ta_{10}$	As cast	BCC	[35]
VAC+ Doped oxygen	$Ti_{40}Zr_{25}Nb_{25}Ta_{10}O_{0.5}$	As cast	BCC	
VAC+ Doped oxygen	$Ti_{40}Zr_{25}Nb_{25}Ta_{10}O_{1.0}$	As cast	BCC	
VAC+ Doped oxygen	$Ti_{40}Zr_{25}Nb_{25}Ta_{10}O_{2.0}$	As cast	BCC	
Ball milling + Spark plasma sintering	$Ti_{53}Zr_{35}Nb_7Ta_5$	Sintered	BCC	[36]
Ball milling + Spark plasma sintering	$Ti_{53}Zr_{35}Nb_7Ta_5$+ 0.25 hBN	Sintered	bcc+α(Ti,N)+TaB_2	
Ball milling + Spark plasma sintering	$Ti_{53}Zr_{35}Nb_7Ta_5$+ 0.5 hBN	Sintered	bcc+α(Ti,N)+TaB_2	
Ball milling + Spark plasma sintering	$Ti_{53}Zr_{35}Nb_7Ta_5$+ 0.1 hBN	Sintered	bcc+α(Ti,N)+TaB_2	
Arc melting	$Ti_{25}Zr_{25}Nb_{25}Ta_{25}$	As cast	BCC	[37]
Arc melting	$Ti_{25}Zr_{25}Nb_{25}Ta_{25}$	annealing (1200°C, 24 h)	BCC1+BCC2	
Cold crucible levitation melting + homogenization + rolling + recrystallization	$Ti_{48.9}Zr_{32}Nb_{12.6}Ta_{6.5}$	Solution-treated	BCC	[38]
	$Ti_{25}Zr_{25}Nb_{25}Ta_{25}$	Deformed	bcc+{112}<111> twin+ω (interfacial)	
VAC	NbZrTiTa	annealing at 1300°C / 2 h	BCC+HCP	[39]
VAC	NbZrTiTa	Hot-compressed 900–1200°C,	BCC+ Dynamic recrystallization (DRX) grain	
Mechanical alloying + Spark plasma sintering	NbZrTiTa	Sintered at 700–1100°C	BCC	[40]
Laser metal deposition (LMD)	$Ti_{25}Zr_{25}Nb_{25}Ta_{25}$	As-built	BCC	[24]
Laser metal deposition (LMD)	$Ti_{25}Zr_{25}Nb_{25}Ta_{25}$	As-built	BCC1+BCC2	
VAM+ Cu mould casting	$Ti_{25}Zr_{25}Nb_{25}Ta_{25}$	AS cast	BCC	[24]

Table 2. Mechanical properties of bone, various bio alloys, and TiZrNbTa Bio-HEAs

Material classification	Specific material	Young's modulus, GPa	Yield strength, MPa	Ductility, %	References
Hard tissue	Cortical bone	10-30	30-70	1.1	[47]
	Cancellous bone	0.01-1.57	4-12	7.1	[48]
Conventional alloys	Ti–6Al–4V	110-120	850-1034	10–15	[49]
	Co–Cr–Mo alloys	210-253	448-1606	8–15	
	316L stainless steel	200-215	221-1213	12–56	
TiZrNbTabio-HEAs	TiZrNbTa (equimolar)	89-116	957-1107	23–36	[27, 31]
	Ti_9Zr_9NbTa (Ti-rich)	57	690	24	[27]
	$Ti_{45}Zr_{45}Nb_5Ta_5$	59.3	626.7	20	
	$Ti_{40}Zr_{40}Nb_5Ta_{15}$	73.1	990	19	
	$Ti_{35}Zr_{15}Nb_{25}Ta_{25}$	91	842	17	[50]
	$Ti_{42.5}Zr_{42.5}Nb_5Ta_{10}$	62.5	786.5	16	

Xiang et al. [25] investigated the effect of heat treatment on the mechanical properties of equiatomic TiZrNbTa HEA. The mechanical behaviour was strongly influenced by thermally induced microstructural evaluation. The compressive yield strength increased with annealing temperature, reaching a maximum value of 1583 MPa after annealing at 600°C for 1h. The alloy exhibited a uniform strain of 20.5±1.8%, representing an improvement of 47% compared with the as-cast condition. Both microhardness and yield strength initially increased and then decreased with increasing annealing temperature, indicating a strong relationship between microstructure and mechanical performance.

The strength enhancement observed at 600°C was attributed to the formation of nanoscale spinodal decomposition structures within the BCC matrix, which increased resistance to dislocation motion. In contrast, the reduction in strength at 700-800°C was associated with the formation of vein-like grain boundary phases. These findings demonstrate that controlled heat treatment is an effective approach for optimizing the strength-ductility balance in TiZrNbTa-based Bio-HEAs.Mustafi et al. [50] investigated a non-equiatomic $Ti_{35}Zr_{15}Nb_{25}Ta_{25}$ alloy and exhibited a single-phase BCC structure. In the cast condition, the alloy achieved a tensile yield strength of 842 MPa, an ultimate tensile strength of 873 MPa, and 17% elongation. These values exceed the minimum strength and ductility requirements of conventional medical grade Ti–6Al–4V alloys. The improved ductility was attributed to reduced atomic mismatch, which promoted plastic deformation through the formation of micro shear bands while suppressing deformation twinning. Furthermore, the alloy maintained a relatively low elastic modulus of 91 GPa, thereby improving mechanical compatibility with bone tissue while preserving structural integrity.

The equiatomic NbTaTiZr alloy was fabricated using powder metallurgy by Xiang et al. [40], producing a dual phase BCC microstructure with grain size ranging from 50-500 nm. The sintering temperature had a significant influence on the mechanical performance of the alloy. Hardness increased with increasing sintering temperature, reaching a maximum value of 662 HV at 800°C. The alloy sintered at 1000°C exhibited the most favorable balance of strength and ductility, achieving a compressive yield strength of 2172±47 MPa, a fracture strength of 2274±91 MPa, a plastic strain of 12.8%, and a Young's modulus of 138 GPa. The superior mechanical performance was attributed to the combined effects of ultrafine grain refinement, solid solution strengthening, and controlled phase distribution. However, excessive grain growth at high sintering temperatures resulted in a gradual reduction in strength.

TiZrNbTa-based Bio HEAs represents a highly adaptable class of materials whose mechanical properties can be tailored through compositional design and processing optimization. However, achieving an optimal balance between high strength – ductility trade off remains a significant challenge, commonly referred to as the strength-ductility trade off [58]. Various strengthening mechanisms, including solid-solution strengthening, spinodal decomposition, heterogeneous phase structures, and bimodal grain-size distributions, have demonstrated the ability to enhance strain hardening while maintaining acceptable mechanical compatibility with bone tissue. Overall, the mechanical behavior of TiZrNbTa-based Bio-HEAs is strongly dependent on composition, microstructural characteristics and processing conditions. These alloys generally exhibit yield strengths ranging from approximately 600 MPa to over 2000 MPa while maintaining elastic modulus values significantly lower than those of conventional biomedical alloys. This unique combination of high strength, relatively low elastic modulus, and good ductility provides significant opportunities for improving the reliability and long-term performance of biomedical implants [27, 36]. Furthermore, the incorporation of alloying elements and the application of advanced processing techniques offer effective strategies for tailoring mechanical performance to meet specific biomedical requirements [59].

3.3. Alloying additions in TiZrNbTa Bio HEAs

The TiZrNbTa alloy system has emerged as one of the most important platforms for the development of Bio HEA because it generally forms a stable single BCC structure and is composed of biocompatible elements [58, 60]. Although the base TiZrNbTa alloy exhibits a promising combination of mechanical and biological properties, further improvements are often required to satisfy the demanding requirements of load-bearing biomedical implants [36, 61]. Consequently, alloying-element additions have become a widely adopted strategy for tailoring phase stability, microstructural evaluation, mechanical performance, corrosion behavior, and biological responses.

The exceptional compositional flexibility of high-entropy alloys enables the incorporation of various metallic elements to achieve specific property enhancements. Alloying additions can influence lattice distortion, solid-solution strengthening, phase formation, passive-film stability, and cellular interactions. As a result, strategic alloy design has become an effective approach for optimizing the multifunctional performance of TiZrNbTa-based Bio-HEAs.

Among the alloying elements investigated, molybdenum (Mo), hafnium (Hf), iron (Fe), aluminum (Al), vanadium (V), nickel (Ni), silver (Ag), and tin (Sn) have received considerable attention because of their ability to modify the microstructure and improve specific properties. The following sections discuss the effects of these alloying additions on phase evaluation, mechanical behavior, corrosion resistance, and biocompatibility in TiZrNbTa-based Bio-HEAs [27, 62, 63].

Molybdenum (Mo) is one of the most extensively investigated alloying elements in TiZrNbTa-based Bio-HEAs because of its excellent biocompatibility, strong β-phase stabilization ability, and significant contribution to mechanical strengthening. Mo is widely used in conventional biomedical alloys, including Ti–15Mo–5Zr–3Al and Co–Cr–Mo alloys, owing to its favorable combination of mechanical and corrosion-resistant properties [2, 64-66]. Consequently, the incorporation of Mo into TiZrNbTa-based alloys has attracted considerable attention as an effective strategy for tailoring microstructure and enhancing overall performance [67]. Qin et al. [68] investigated the influence of Mo addition on the microstructural evaluation of the non-equiatomic $(Ti_{42.5}Zr_{42.5}Nb_{10}Ta_5)100\text{-}xMox$ (x = 0, 3, 5 and 7 at.%) HEA. As shown in Figure 3a, all alloys exhibited a stable single BCC solid-solution structure that indicating that Mo additions of up to 7 at.% did not form the secondary phase. The gradual change of the BCC diffraction peaks to the higher diffraction angles with increasing Mo ratio suggests a decreasing in the lattice parameter caused by lattice distortion. SEM images of (Figure 3b-c) presented a typical dendritic microstructure in both the Mo-free and Mo-containing alloys. However, the size of dendrite became progressively decreased as the Mo content increased. Electron backscatter diffraction (EBSD) analysis (Figure 3d–e) confirmed that all alloys maintained equiaxed BCC grains, with the average grain size decreased from 31.26 μm to 15.57 μm as the Mo content increased from 0 to 7 at.%. Additionally, the kernel average misorientation (KAM) maps and statistical analysis (Figure 3f) showed an increase in the average KAM value from 0.1956° to 0.2934°, indicating enhanced lattice distortion and local strain.

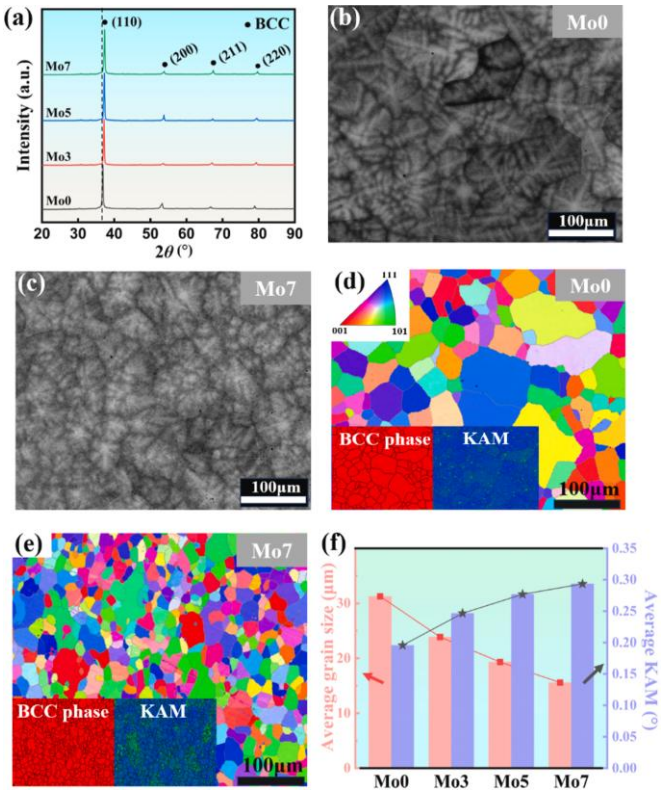


Figure 3. (a) XRD patterns of the $(Ti_{42.5}Zr_{42.5}Nb_{10}Ta_5)100\text{-}xMox$ (x = 0, 3, 5 and 7 at.%) HEAs; (b ~ c) SEM images of the Mo0 and Mo7 RHEAs, (d ~ e). EBSD analyses of the Mo0 and Mo7 HEAs, (f) Average grain size and KAM value of the Mo0 - Mo7 HEAs [68]

These findings demonstrate that Mo addition effectively refines the grain structure and increases lattice distortion while preserving the single-phase BCC microstructure, thereby providing a favorable microstructural basis for strengthening. However, higher Mo concentrations in

equiatomic TiZrNbTaMo systems with high molar ratio of Mo promote the formation of dual BCC structure, namely BCC1+BCC2 accompanied by pronounced dendritic segregation [65]. During solidification, high melting point elements such as Ta, Nb, and Mo preferentially partition into dendritic regions, whereas Ti and Zr were enriched in interdendritic regions [60]. This segregation behavior arises from differences in melting temperature, atomic size, and thermodynamic interactions between the constituent elements.

Ishimoto et al. [69] investigated the selective laser melting (SLM) processed Ti1.4Nb0.6Ta0.6Zr1.4Mo0.6 HEA and reported a porosity below 0.5 %. Owing to the rapid cooling rate of SLM process, severe elemental segregation was largely suppressed, resulting in a relatively homogeneous BCC structure. Microstructural Characterization revealed that Ti and Zr remained concentrated in inter-dendrite region, while Nb, Ta, and Mo were enriched in the dendrite region. Additionally, low Mo concentration reduced the lattice parameter difference between the BCC phases, and making their structures more similar while maintaining chemical heterogeneity [23].

The primary strengthening mechanism associated with Mo addition is solid-solution strengthening. The relatively small atomic radius and high shear modulus of Mo generate significant lattice distortion and modulus-misfit strengthening effects within the BCC matrix [23, 70]. Qin et al. [68] reported that addition of 5 at. % Mo increases the yield strength from 703 MPa to 925 MPa while maintaining a tensile ductility of 21.8% [68]. Similarly, Wang et al. [65] reported a compressive yield strength of 1390 MPa for Mo containing TiZrNbTa alloys, substantially exceeding values predicted by conventional rule-of-mixtures calculations. Aranda et al. [23] directly compared TiNbZrTa alloy and Mo containing TiNbZrTa alloy. The TiNbZrTa alloy exhibited the dendritic BCC structure and demonstrated that Mo addition refined the dendritic microstructure and reduced the lattice-parameter difference between dendritic and interdendritic regions. Consequently, yield strength increased from 940 MPa to 1546 MPa, microhardness increased from 281 HV to 399 HV and elastic modulus increased from 110 GPa to 200 GPa. These findings confirm that Mo addition may increase alloy stiffness, potentially reducing mechanical compatibility with bone tissue.

Powder metallurgy studies have also demonstrated the beneficial effects of Mo addition. Shkodich et al. [72] reported that Mo promoted the formation of a refined multiphase BCC structure with enhanced lattice distortion, resulting in hardness values of up to 8.5 GPa and comprehensive strength of 1625 MPa. Furthermore, Akmal et al. [73] investigated (MoTa)xNbTiZr HEAs and found that low Mo–Ta content favored a single BCC phase, whereas higher concentrations of Mo ($x \geq 0.8$) promoted dual BCC structures. Increasing Mo and Ta contents improved hardness and yield strength increased significantly, whereas ductility gradually decreased and elastic modulus increased, indicating a trade-off between mechanical strength and biomechanical compatibility [57].

The addition of molybdenum (Mo) is crucial for enhancing the properties of TiZrNbTa-based Bio-HEAs. Mo contributes to solid-solution strengthening, lattice distortion, and microstructural refinement. A moderate amount of Mo provides an effective balance between strength and ductility while ensuring good corrosion resistance and biocompatibility. However, excessive Mo concentrations can lead to an increased elastic modulus, which may reduce compatibility with bone tissue. Therefore, optimizing the Mo content is essential to achieve the desired combination of mechanical and biological properties in TiZrNbTa-based Bio-HEAs. Table 3 summarizes the microstructural and mechanical effects of Mo addition in TiZrNbTa-based Bio-HEAs.

Table 3. Microstructure and mechanical properties of TiZrNbTaMo BIO HEAs

Alloy	Microstructure	Hardness, GPa	Young's modulus, GPa	Yield strength, MPa	Reference
$Ti_{20}Zr_{20}Nb_{20}Ta_{20}Mo_{20}$	BCC1+BCC2	4.9 GPa	153	1390	[65]
$(TiZrNbTa)_{80}Mo_{20}$	BCC1+BCC2	4.9±0.1	155±6	1460±40	[70]
$(TiZrNbTa)_{85}Mo_{15}$		4.5±0.1	150±3	1370±60	
$(TiZrNbTa)_{90}Mo_{10}$		4.2±0.1	137±3	1300±30	
$(TiZrNbTa)_{95}Mo_{5}$		3.7±0.1	129±3	1180±30	
$(TiZrNbTa)_{100}$		3.2±0.1	115±3	1020±10	
TaTiNbZrMo	BCC1+BCC2	5.1±0.4	-	1480	[72]
TaTiNbZrMo	BCC+ Nano crystalline	8.5±0.1	-	-	
$(Ti_{42.5}Zr_{42.5}Nb_{10}Ta_5)_{93}Mo_7$	Single BCC	4.93± 0.28	129±3.19	975	[68]
$(Ti_{42.5}Zr_{42.5}Nb_{10}Ta_5)_{95}Mo5$		4.44± 0.22	117±2.43	923	
$(Ti_{42.5}Zr_{42.5}Nb_{10}Ta_5)_{97}Mo3$		3.40±0.51	111±4.59	828	
$(Ti_{42.5}Zr_{42.5}Nb_{10}Ta_5)100$		2.33±0.30	103±2.81	670	
$(Ti_{42.5}Zr_{42.5}Nb_{10}Ta_5)100\text{-}x\ Mox\ (x = 5)$	Single BCC	292.0±10.7	-	925±6.4	[68]
$(Ti_{42.5}Zr_{42.5}Nb_{10}Ta_5)100\text{-}x\ Mox\ (x = 0)$		229.4±11.5	-	703±14.5	
MoNbTaTiZr	BCC	6.45±0.06	164.06±1.70		[74]
$Ti_{35}Zr_{15}Nb_{25}Mo_{15}Ta_{10}$	BCC1+BCC2	590HV	124	810±31	[75]
$Ti_{27}Nb_{33}Zr_2Mo$	BCC	244±8 HV	73±3	695	[76]
$Ti_{30}Nb_{28}Zr_2Mo$	BCC	235±6 HV	70±5	678	
$Ti_{24}Nb_{38}Zr_2Mo$	BCC	239±6 HV	68±1	675	
$Ti_{37}Nb_{16}Zr_2Mo$	BCC	220±6 HV	72±2	584	

Hafnium (Hf) has attracted considerable attention as an alloying element in TiZrNbTa based Bio HEAs because of its excellent biocompatibility, large atomic radius and a strong lattice distortion strengthening effect [77, 78]. As a group-IV transition metal with chemical properties similar to Zr, Hf is considered biologically safe and exhibits excellent corrosion resistance in physiological environments. Furthermore, Hf can improve phase stability and mechanical performance while maintaining the biocompatibility required for biomedical implant applications [79-80].

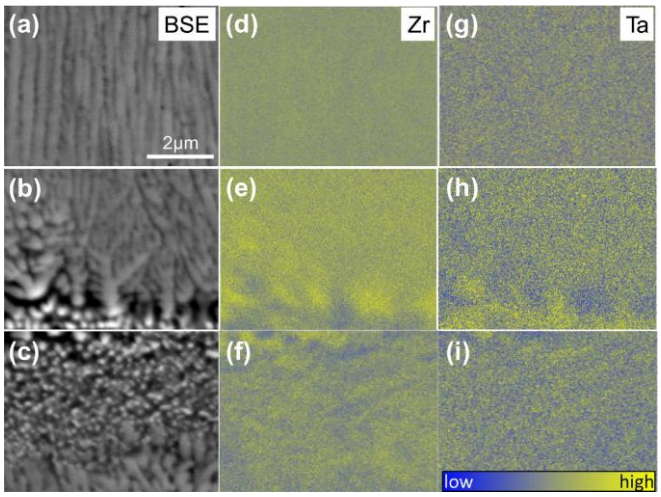


Figure 4. SLMed BioHEA specimen Ti1.4Nb0.6Ta0.6Zr1.4Mo0.6. (a–c) BSE pictures, (d–f) Zr EDS maps, and (g–i) Ta EDS maps. The small concentration difference suggests that SLM significantly inhibited elements segregation. To make a small concentration variation visible, the EDS pictures are presented with high contrast [69]

The same composition of arc melted TiNbZrHfTa alloys were investigated by Gurel et al., [81], Yang et al., [82] and Berger et al. [83] who reported single phase BCC microstructure with homogeneous elemental distributions. The influence of Hf on deformation behavior of equimolar TiZrNbTaHf HEA is reported by Eleti et al. [84] and alloy exhibited a stable single-phase BCC microstructure (grain size ranging from 10 to 60 μm). The alloy exhibited strong temperature dependent mechanical behavior, with yield strength increasing from 984 MPa at 300 K to 1638 MPa at 77 K. This improvement was attributed to stable BCC phase formation and increased resistance to dislocation motion at low temperature.

High-pressure torsion (HPT) process can improve the mechanical properties of Hf containing TiZrNbTa-based alloys. Hruška et al. [85] reported that high-pressure torsion (HPT) processing of TiNbZrTaHf alloy preserved the BCC structure while producing significant grain refinement. The processed alloy exhibited a hardness of approximately 564 HV and an elastic modulus of 79±3 GPa. Similarly, Málek et al. [86] investigated the SPS processed TiZrNbTaHf HEA followed by HPT. The processed alloy exhibited a refined BCC structure, a grain size of 500 nm and hardness of 410 HV. These studies demonstrate the Hf containing Bio HEA with HPT technique can enhance the microstructure and mechanical properties.

Using thermodynamic model, Ding et al. [87] predicted that TiZrNbTaHf HEA can maintain single BCC phase structure over a wide compositional range. However, reduced concentration in Nb and Ta content may promote the formation of BCC+HCP dual phase structures, indicating that phase stability is highly dependent on elemental composition. Experimental observations by Cao et al. [34] confirmed these predictions. In homogenized conditions, equiatomic TiZrNbTaHf HEA exhibited a single-phase BCC structure in initial stage. After heat treatment at 500-600°C, the alloys resulted in the precipitation of HCP within BCC phase matrix. At 650-1000°C, the alloy developed a multiphase microstructure consists of two BCC phases and one HCP phase that indicates elemental partition between Ta/Nb-rich and Hf/Zr-rich regions.

Yuan et al. [88] investigated a series of TiZrHfNbTa HEA and demonstrated that most compositions exhibited stable BCC structures. However, mixed HCP+BCC phases were observed in TaxNbxHfZrTi (x = 0.2) HEA. Elemental segregation was observed, with Nb and Ta dendritic re-gions and Ti and Zr enriched in interdendritic regions. Mechanical properties varied significantly with composi-tion modifications; young's modulus ranged from 57 to 135 GPa and the yield strength is 690-1050 MPa that demonstrate the composition can affect the mechanical behavior of Hf-containing Bio-HEAs. Also, Dobbelstein et al. [89] printed the TiZrNbHfTa HEA using laser metal deposition (LMD) technique. The alloy exhib-ited the single BCC phase; however, a minor HCP phase was observed near substrate interface because of compositional mixing during deposition. From all these findings, Hf addition in TiZrNbTa-based Bio HEAs promotes the formation of a stable BCC solid solution microstructure under suitable compositional and processing conditions. Although, secondary HCP phases may form under specific heat treatment, or compositional variations. Hf-containing TiZrNbTa-based Bio-HEAs generally exhibit a favorable combination of phase stabil-ity, microstructure, and mechanical properties in TiZrN-bTa(Hf)-based Bio-HEAs.

In addition to Mo and Hf, the researchers have investigated various alloying elements including nickel (Ni), aluminum (Al), iron (Fe), vanadium (V), and silver (Ag) to further tailor the properties of TiZrNbTa-based Bio HEAs. These alloying additions are primarily employed to optimize the balance between high yield strength, ductility, and low elastic modulus, which are critical factors for biomedical implant applications. Through solid-solution strengthening, phase transformation, precipitation strengthening, and microstructural refinement, these elements can significantly influence the mechanical and functional performance of TiZrNbTa-based alloys.

The addition of **Aluminum (Al)** in TiZrNbTa alloy can promote microstructural refinement, spinodal decomposition and improved ductility balance. In $(TiZrNbTa)_{98.5}Al_{1.5}$ HEA, the addition of Al resulted in the formation of a basket weave morphology with characteristic periodicity of 8 nm. The microstructural feature increased the tensile strength to 1045 MPa and ductility to 21.5%. Furthermore, increasing the Al content to 2.4% promoted the formation of brittle intermetallic phases and reduced plasticity formation capability [90].

Wang et al. [91] developed the **Iron (Fe)** containing TiZrHfNbFex (x = 0, 0.25, 0.5, 0.75, 1, 1.5, and 2, molar ratio) refractory Bio-HEAs to investigate the influence of Fe addition on microstructural evaluation and mechanical performance. The Fe-free TiZrHfNb alloy exhibited a single BCC solid-solution structure, whereas the introduction of Fe promoted the formation of a dual-phase microstructure consisting of BCC and Fe_2Nb Laves phases. With increasing Fe content, the fraction of the Laves phase gradually increased, accompanied by dendritic refinement and enhanced lattice distortion. As a result, hardness increased continuously from approximately 320 HV for the Fe-free alloy to about 770 HV for the Fe_2 alloy. Among the investigated compositions, $TiZrHfNbFe_{0.5}$ exhibited the best combination of strength and ductility, achieving a hardness of approximately 420 HV, a compressive strength of 1450 MPa, and a plastic strain of about 8%. However, further increases in Fe content led to excessive Laves-phase formation and a significant reduction in plasticity due to the brittle nature of the intermetallic phase.

Similarly, Popescu et al. [53] investigated the $Ti_{40}Nb_{20}Zr_{20}Ta_{10}Fe_{10}$ HEA via a powder metallurgy route and reported the formation of a β-phase BCC microstructure with improved hardness, mechanical performance and enhanced corrosion resistance. These findings demonstrate that adding Fe is an effective method for enhancing the strength and hardness of TiZrNbTa-based alloys; however, precise control of composition is necessary to prevent excessive embrittlement due to secondary-phase formation.

The addition of **Vanadium (V)** in TiZrNbTa alloy exhibited a homogeneous BCC microstructure while enhancing mechanical strength. V-containig TiZrNbTa-based Bio HEAs revealed dendritic segregation with Nb and Ta preferentially partitioning into dendritic regions and Ti, Hf, and V enriched in interdendritic regions. Reported alloy exhibited a yield strength of 1350 MPa while maintaining 45% of tensile ductility which represents a 50% improvement compared with similar HfNbTaTiZr HEA [78]. Similar segregation behavior has been observed in the equiatomic $Nb_{20}Ta_{20}Ti_{20}V_{20}Zr_{20}$ HEA. Du et al. [26] reported a BCC dendritic microstructure with an average grain size of approximately 84.7 μm. During the solidification process, Ta and Nb preferentially segregated into the dendritic regions, while Zr was enriched in the interdendritic areas. Additionally, Ta-rich cubic and elliptical nanoprecipitates were found along the grain boundaries in Zr-rich regions. These findings indicate that thermodynamically driven elemental partitioning and diffusion kinetics play crucial roles in influencing phase separation and the microstructural evaluation of vanadium (V) containing refractory HEAs.

The minor addition of **Nickel (Ni)** can promote the heterogeneous microstructures consisting of dual BCC phase with minor HCP constituents. The $TiZrNbTaNi_{0.05}$ alloy exhibited a yield strength of 1135 MPa, an ultimate tensile strength 1235 MPa, and an elongation of 22%. The enhanced mechanical performance can be attributed to precipitation strengthening and hetero-deformation-induced strain hardening linked to the multiphase microstructure. These findings show that small additions of nickel (Ni) can effectively improve both strength and ductility. However, since nickel is often regarded as a potential allergenic element in biomedical applications, its concentration must be carefully regulated to minimize biological risks while still achieving the desired mechanical advantages [58].

Silver (Ag) has garnered interest as an alloying element in TiZrNbTa-based Bio-HEAs because of its well-known antibacterial properties and potential to enhance implant performance. Besides providing antimicrobial activity, Ag can also influence phase formation and microstructural evaluation. A non-equiatomic 35Ti–35Zr–20Nb–5Ta–5Ag alloy system was fabricated using a powder metallurgy route and exhibited a single BCC structure after sintering. After SPS at 1300^0C the phase separation was observed, resulting in a dual BCC phase microstructure with the formation of ultrafine Zr-rich equiaxed phase contained 2.3 at. % Ag. Elemental analysis revealed Ag enrichment at grain boundaries of up to 21.4 at.% also observed along BCC2 grain boundaries. The Ag containing alloy exhibited an elastic modulus of 84.4 to 113.2 GPa and microhardness value of 3.47 to 5.35 GPa, indicating a favorable mechanical profile. The addition of elements such as Fe, V, Ni, and Ag provides effective strategies to tailor the microstructure and mechanical performance of TiZrNbTa-based Bio-HEAs. Fe enhances strength primarily through precipitation strengthening and the formation of Laves phases. V contributes to strength via solid-solution strengthening and lattice distortion. Ni promotes strengthening through heterostructuring and enhances strain-hardening capability, while Ag adds antibacterial properties without significantly compromising mechanical performance. These findings highlight that the selection of alloying elements is crucial for balancing strength, ductility, elastic modulus, corrosion resistance, and biological compatibility. Therefore, rationally designing alloying additions is an essential strategy for developing next-generation TiZrNbTa-based biomedical high-entropy alloys. Table 4 summarizes the reported effects of various alloying elements on the microstructural and mechanical properties of TiZrNbTa-based Bio HEAs.

Table 4. Effect of adding other elements in TiZrNbTa alloy

Element	Microstructure evaluation	Strength changes	Strengthening mechanism
Mo	Single BCC to dual BCC1 + BCC2 with compositional changes	Increase in yield strength and hardness	Solid-solution strengthening, lattice distortion, and phase separation
Hf	Maintain stable BCC phase; possible BCC + HCP at certain compositions with heat treatment	Moderate strength improvement	Atomic size mismatch strengthening and phase stabilization
Fe	Formation of BCC matrix with laves intermetallic phase	Improve mechanical properties and hardness	Intermetallic formation and strong lattice distortion from small Fe elements
Al	Formation of spinodal structure and ordered B2 phase within BCC matrix	Improved strength–ductility balance	Spinodal decomposition strengthening, chemical ordering
Ni	Multi heterostructure with dual BCC phases and secondary phases like HCP	Increase in Yield strength and ductility	Hetero deformation and induced strengthening
V	Maintains single BCC phase	Improve mechanical properties with improved ductility	solid solution strengthening and atomic size mismatches
Ag	Retains BCC structure and minimal phase change raising temperature	Development in mechanical properties	microstructural stability
Ta (increase)	Stabilizes BCC phase	Improve mechanical strength	Strong atomic bonding, lattice distortion
Ti / Zr (increase)	Stabilizes BCC	Relative decrease in strength/stiffness	Reduced stiffness and lattice softening

4. Corrosion properties of TiZrNbTa based BIO HEAs

Corrosion remains one of the major challenges affecting the long-term performance of metallic implant materials in biomedical applications because it can compromise implant performance and pose potential risk for patient health. The degradation of implant materials may release the metallic ions into surrounding tissues, potentially causing inflammatory reactions and other adverse biological responses [10, 92]. Consequently, excellent corrosion resistance is one of the most important requirements for biomedical alloys. After implantation, metallic materials are exposed to complex physiological environments containing chloride ions, metal ions, proteins, organic compounds and various electrolytes at approximately 37°C. These factors can significantly influence the electrochemical behavior and long-term stability of implant materials [4, 93, 94, 95].

TiZrNbTa-based Bio-HEAs have received significant attention because of their capacity to create thick, adherent, and stable passive oxide films that effectively protect the alloy surface from corrosion [95].

The following key studies illustrate the electrochemical behavior and corrosion resistance of TiZrNbTa Bio HEA. Guo et al. [96] investigated the effect of Ta on corrosion behaviour of $ZrTiHfTa_x$ (x = 0.25, 0.5, 0.75, and 1) alloy. Increasing the Ta concentration progressively improved the corrosion resistance through enhanced passive film stability. Electrochemical measurements showed the reduction in current density with increasing Ta content, while the polarization behaviour indicated improvement passivation performance. The improved performance was attributed to the enrichment of Ta_2O_5 within the passive film, which reduced defect density and promoted the formation of a denser protective oxide layer. Wang et. al. [97] investigates the corrosion behavior of $Ti_{1.6}ZrNbMo_{0.35}$ HEA in 3.5 wt.% NaCl solution and reported excellent corrosion resistance characterized by a stable passive region and low corrosion current density. The enhanced corrosion resistance was attributed to the formation of mixed passive oxides and the presence of Mo^{6+} species, which significantly improved pitting corrosion resistance and passivation stability. The addition of Mo promoted continuous passive film formation and increased charge transfer resistance, thereby improving the corrosion resistance in TiZrNb-based Bio HEAs.

Similarly, TiZrNbTaMo HEAs showed superior electrochemical performance compared with Ti–6Al–4V, Co–Cr–Mo alloys, and 316L stainless steel, exhibiting stable passive behavior without evidence of localized corrosion [65].

Yang et al. [82] investigated equiatomic TiTaHfNbZr HEA and reported excellent passivation behavior in simulated physiological environment. The alloy exhibited a low corrosion current density of 0.08×10^{-2} A/M-2 and a corrosion rate of 5.6×10^{-4} mm/year^{-1} outperforming conventional Ti-6Al-4V. The superior corrosion resistance was attributed to the formation of a highly stable passive film composed of TiO_2, ZrO_2, HfO_2, Nb_2O_5, and Ta_2O_5. Wang et al. [91] evaluated the corrosion behavior of TiZrHfNbFex (x = 0-2) HEA in phosphate-buffered saline (PBS) solution and revealed that $TiZrHfNbFe_{0.5}$ exhibited the lowest corrosion current density (2.80×10^{-7} A cm^{-2}) and superior corrosion resistance compared with Ti–6Al–4V and the other TiZrHfNbFex alloys. The enhanced corrosion performance was attributed to the formation of stable passive oxide films composed primarily of TiO_2, ZrO_2, HfO_2, Nb_2O_5, and Fe_2O_3, which effectively reduced ion dissolution and improved surface protection. However, when the Fe content exceeded x = 1, corrosion resistance gradually deteriorated because of increased phase heterogeneity and the development of micro-galvanic corrosion [53].

The corrosion behaviour of $(Ti_{42.5}Zr_{42.5}Nb_{10}Ta_5)100$-xMox (x = 0, 5) HEA was evaluated in PBS and SBF solution [61]. The alloy with Mo-free alloy (x = 0) exhibited the lowest corrosion current density of 1.02×10^{-7} A/cm^{-2} in PBS solution and 0.91×10^{-7} A/cm^{-2} in simulated body fluid (SBF) solution. The Mo 5 at.% alloy exhibited higher current density values of 1.23×10^{-7} A/cm^{-2} in PBS solution and 2.13×10^{-7} A cm^{-2} in SBF solution. The electrochemical response of Mo (x = 0, 5),CP-Ti, and TC4 alloys. The Tafel curves exhibited broad passive regions without abrupt increases in current density, indicating the formation of stable passive films on all investigated alloys. The Nyquist plots display larger capacitive arc diameters for the HEAs than for CP-Ti and TC4, reflecting higher polarization resistance and improved corrosion resistance. Consistent with the Tafel results, the Mo-free alloy exhibited the highest polarization resistance and impedance, indicating a more protective passive film. Furthermore, bode plots reveal high phase angles, confirming the presence of a dense and stable passive oxide layer. These results suggest that 5 at.% Mo slightly reduced the corrosion resistance compared with the Mo-free alloy.

The corrosion resistance of Bio HEA has been evaluated in various physiological environments using various chemical solutions like phosphate buffer solution (PBS), fetal bovine serum (FBS), Ringer's solution, Hank's solution, simulated body fluid (SBF), NaCl solution Table 5 summarizes the corrosion parameters of the TiZrNbTa based Bio HEAs in these environments.

Overall, TiZrNbTa-based Bio HEAs exhibits excellent corrosion resistance in physiological environments owing to the formation of stable passive oxide films composed of TiO_2, ZrO_2, Nb_2O_5, Ta_2O_5. Additional oxide such as MoO_2 or HfO_2 further enhance passivation behavior by improving oxide film stability and reducing defect density. These layers of protection improve long term electrochemical stability and biocompatibility under physiological conditions. TiZrNbTa-based Bio-HEAs exhibit notable advantages over conventional biomedical alloys such as Ti–6Al–4V, Co–Cr–Mo, and 316L stainless steel. They typically show lower corrosion current densities, wider passive regions, and enhanced electrochemical stability. These traits help minimize the release of metallic ions and promote long-term biocompatibility. As a result, TiZrNbTa-based Bio-HEAs are considered promising candidates for next-generation biomedical implant applications.

5. Biocompatility of TiZrNbTa based Bio HEAs

The revised literature [36, 51, 73, 74, 75, 82, 101, 109-114] on TiZrNbTa-containing high-entropy or multi-principal-element alloys generally demonstrate good biocompatibility and low cytotoxicity. These alloys are particularly promising when contain biologically accepted elements such as Ti, Zr, Nb, Ta, Hf, and, in some cases, Mo or Sn. Most studies report favorable cell responses, including enhanced adhesion, viability, and proliferation of osteoblast-like cells. However, the biological performance of these alloys is influenced not only by their chemical composition but also by their surface characteristics. Improved cellular responses are commonly associated with the formation of stable passive oxide films, increased surface wettability, and surface modifications, including annealed microstructures, nanotubular oxide coatings, and sputtered nanostructured films. These surface features improve the biological response of cells to the alloy surface, contributing to better osseointegration. However, most studies focused only on in vitro cytocompatibility, while studies on immune responses, long-term osseointegration, and in vivo bone performance remain limited [82, 110, 113, 114].

The biocompatibility of TiZrNbTa implant candidates can be divided into three main categories. The first is chemical biocompatibility, which is characterized by the formation of a stable passive surface that minimizes the release of potentially harmful metal ions under physiological conditions.

Table 5. Electrochemical properties for TiZrNbTa based HEAs

Bio-HEA	Solution	E_{corr} (V)	I_{corr}	Reference
$TiZrHfNbFe_{0.75}$	PBS	−0.27±0.01	1.66±0.27×10^{-7} A/cm^2	[91]
$TiZrHfNbFe_1$	PBS	−0.33±0.02	5.18±1.81×10^{-7} A/cm^2	
$TiZrHfNbFe_0$	PBS	−0.39±0.03	10.93±2.77	
$TiZrHfNbFe_{0.5}$	PBS	−0.30±0.01	2.80±0.77	
$TiZrHfNbFe_{0.25}$	PBS	−0.42±0.05	2.80±0.77	
$TiZrHfNbFe_{1.5}$	PBS	−0.49±0.04	15.5±0.25×10^{-7} A/cm^2	
$TiZrHfNbFe_2$	PBS	−0.51±0.01	27.1±2.21×10^{-7} A/cm2	
TiNbTaZr	PBS	−0.42	19±0.15	[32]
$Ti_{1.6}ZrNbMo_{0.35}$	3.5 wt.% NaCl	−0.409	4.57μA/cm^2	[97]
TiZrNbTaMo	PBS	−0.465	0.0.017μA/cm^2	[62]
$(TiZrNb)_{14}SnMo$	SBF	−0.85	2.01× 10^{-6} A/cm^2	[99]
TiZrHfNb	PBS	−0.38	1.08×10^{-6}	[91]
$TiZrHfNbFe_{0.5}$	PBS	−0.30	2.80×10^{-7}	
$Ti_{25}Nb_{10}Ta_1Zr_{0.2}Fe$	Ringer's solution	−0.071.7	0.22 μA/cm^2	[100]
$(Ti_{0.2}Zr_{0.2}Hf_{0.2}Nb_{0.2}Ta_{0.2})$100-xSn0	Hank's solution	–0.395±0.008	0.08±0.10	[101]
$(Ti_{0.2}Zr_{0.2}Hf_{0.2}Nb_{0.2}Ta_{0.2})$100-xSn3	Hank's solution	–0.456±0.016	0.21±0.02	
$(Ti_{0.2}Zr_{0.2}Hf_{0.2}Nb_{0.2}Ta_{0.2})$100-xSn5	Hank's solution	–0.484±0.011	0.18±0.05	
$(Ti_{0.2}Zr_{0.2}Hf_{0.2}Nb_{0.2}Ta_{0.2})$100-xSn7	Hank's solution	–0.458±0.012	0.30±0.01	
$Ti_{40\cdot5}Zr_{25\cdot3}Nb_{25\cdot3}Mo_{8.9}$	3.5 wt.% NaCl solution	-0.409	4.57 μA/cm^2	[97]
TiZrNbHfSi	Ringer's solution	−0.330 V	0.08 μA/cm^2	[102]
$Ti_{20}Zr_{20}Hf_{20}Nb_{20}Ta_{20}$	Hank's solution	−0.302±0.014	0.08×10^{-7} A/cm^2	
$Ti_{35}Nb_2Ta_3Zr$	SBF	−0.339	0.205 μA/cm^2	[103]
TiZrHfNbTa	Hank's solution	−0.395±0.008	0.08±0.01A/cm^2	[82]
$(TiZr)_{75}Nb_{15}Mo_{10}$	SBF	−0.317	74.2 μA/cm^2	[104]
Mo0 ($Ti_{42.5}Zr_{42.5}Nb_{10}Ta_5$)	PBS	−0.25±0.005	1.02±0.031×10^{-7} A/cm^2	[61]
Mo_5 ($Ti_{42.5}Zr_{42.5}Nb_{10}Ta_5)_{95}Mo_5$	PBS	−0.53±0.006	1.23±0.022×10^{-7} A/cm^2	
Mo_0 ($Ti_{42.5}Zr_{42.5}Nb_{10}Ta_5$)	SBF	−0.43±0.010	0.91±0.019×10^{-7} A/cm^2	
Mo_5 ($Ti_{42.5}Zr_{42.5}Nb_{10}Ta_5)_{95}Mo_5$	SBF	−0.47±0.012	2.13±0.038×10^{-7} A/cm^2	
$Ti_{20.6}Nb_{13.6}Zr_{-0.5}V$	Ringer's solution	−0.171	0.777 μA/cm^2	[18]
TiZrNbTaFe	Ringer's lactate	−0.071.7	0.22μA/cm^2	[53]
$Ti_{40}Zr_{40}Nb5Ta_{12}Sn_3$	Artificial saliva	−0.31420	2.613×10^{-7} A/cm^2	[105]
$Ti_{40}Zr_{40}Nb5Ta_{12}Sn_3$	Simulated blood	−0.33999	4.932×10^{-7} A/cm^2	
(Ti0.2Zr0.2Hf0.2Nb0.2Ta0.2)97Sn3	Hank's solution	−0.456	0.21× 10^{-3} A/m^2	[101]
TiZrHfNbTa	Hank's solution	−0.395	0.80× 10^{-2} A/m^2	[82]
$Ti_{1.5}ZrTa_{0.5}Nb_{0.5}W_{0.5}$	Hank's solution	−0.160	0.089μA/cm^2	[106]
$Ti_{20}Zr_{20}Hf_{20}Nb_{20}Ta_{20}$	Hank's solution	−0.302	0.08× 10^{-3} A/m^2	[107]
35Ti–35Zr–20Nb–5Ta–5Ag -700 MPa	SBF	−0.182	0.068μA/cm^2	[108]
35Ti–35Zr–20Nb–5Ta–5Ag -550 MPa	SBF	−0.125	13.078	
$ZrTiHfTa_{1.00}$	0.05 M NTO	− 540.93±7.83	7.90±0.29 nA/cm^2	[96]
$ZrTiHfTa_{0.71}$	0.05 M NTO	− 568.23±15.45	10.83±0.93 nA/cm$_2$	
$ZrTiHfTa_{0.47}$	0.05 M NTO	− 592.17±17.06	17.47±3.09nA/cm^2	
$ZrTiHfTa_{0.25}$	0.05 M NTO	− 614.67±25.9	20.20±4.77nA/cm^2	

In the reviewed studies, this aspect is primarily evaluated through corrosion testing in Hank's solution, simulated body fluid (SBF), or phosphate-buffered saline (PBS), combined with electrochemical techniques such as open-circuit potential (OCP), potentiodynamic polarization, electrochemical impedance spectroscopy (EIS), and ion-release analysis, as discussed in the previous section. The equiatomic TiZrHfNbTa alloy is a representative example, as X-ray Photoelectron Spectroscopy (XPS) analysis attributed its excellent corrosion resistance and biocompatibility to the formation of stable passive oxides, including TiO_2, ZrO_2, HfO_2, Nb_2O_5, and Ta_2O_5 [82]. The second is cellular biocompatibility which reflects the ability of a material to support cell survival, attachment, spreading, and proliferation. Across the reviewed literature, this is most commonly assessed using MTT or CCK-8 assays, live/dead staining, and microscopic evaluation of cell morphology, including filopodia and lamellipodia formation. The third is mechanical biocompatibility, which focuses on minimizing stress shielding by reducing the elastic modulus to better match of natural bone. This concept is consistently emphasized in the reviewed studies, where low-modulus β-Ti alloys and high-entropy alloys are considered advantageous because excessive implant stiffness can hinder bone remodeling and osseointegration, even in the absence of cytotoxic effects [101, 109, 111].

As summarized in Table 6, the strongest short-term in vitro evidence comes from the TiZrHfNbTa, TiNbTaZrMoV, TiZrHfNbTa nanofilm, and TNZT-hBN composites. TiZrHfNbTa showed no significant difference in the number of adherent MC3T3-E1 cells compared with Ti-6Al-4V after 24 hours, with no dead or unhealthy cells observed after 72 hours. The cells continued to proliferate over time, and the alloy exhibited bio-corrosion resistance comparable to that of Ti-6Al-4V [82]. TNZT-hBN composites processed by SPS also retained excellent cytocompatibility, with cell survival and proliferation exceeding 95% and cell adhesion comparable to that of the unreinforced TiZrNbTa alloy matrix [36]. Similarly, the TiNbTaZrMoV alloy exhibited a PBS contact angle of 77.9±1.6°, which was comparable to that of Ti-6Al-4V (76.6±1.0°). No dead cells were detected by live/dead stain-ing after 3 days of culture, and cell proliferation after 7 days was statistically indistinguishable from that of Ti-6Al-4V [109].

Surface-modified alloys generally exhibited better biological performance than their bulk counterparts. On AISI 316L, the TiZrHfNbTa refractory high-entropy nanofilm showed the highest corrosion potential (−0.127 V), a corrosion current density two orders of magnitude lower than that of the substrate, and an osteoblast proliferative capacity approximately 1.5 times higher than that of the substrate after 5

days. The nanofilm also promoted collagen secretion and extracellular matrix mineralization [113]. Likewise, coral-like metal-oxide nanotubes formed on TiZrNbTa initially reduced cell proliferation after 1 and 4 days compared with the bare TiZrNbTa alloy. However, after 7 days, the modified surface reached an OD value of 2.78, slightly higher than that of the bare alloy, indicating a delayed but favorable cellular response to the micro-/nano-textured surface [114].

The reviewed studies also show that the effect of individual alloying elements is not always consistent. In the TiZr-based RMPEAs, MoTiZr, NbTiZr, and NbMoTiZr supported elongated MC3T3-E1 cell morphologies comparable to those observed on Ti-6Al-4V, whereas the V-containing MoTiVZr and NbTiVZr exhibited smaller, more elliptical cells [112]. However, TiNbTaZrMoV showed better wettability, cell proliferation, and live/dead response than the V-free TiNbTaZrMo alloy [109]. These findings indicate that the biological effect of vanadium depends on the overall alloy composition and microstructure rather than on the presence of V alone.

While the reviewed studies provide encouraging in vitro results, evidence from *in vivo* studies remains scarce. Among the reviewed alloys, $(MoTa)_{0.2}NbTiZr$ demonstrated good corrosion resistance and no adverse tissue response after 4 weeks of implantation in mouse thigh muscle. Although these results are promising, they reflect soft tissue compatibility rather than direct bone integration and osseointegration performance [73].

5.1. Effect of ,anufacturing method on biocompatibility

The reviewed alloys were produced using several manufacturing methods, including arc melting, vacuum arc melting, spark plasma sintering (SPS), mechanical alloying combined with SPS, Direct Current (DC) magnetron sputtering, and cold crucible levitation melting. The available results suggest that the manufacturing method affects biocompatibility indirectly by influencing the surface and microstructural features of the alloy. Changes in oxide layer chemistry, surface roughness, texture, segregation, and nanostructure can alter protein adsorption and subsequent cellular interactions, thereby contributing to differences in biological performance.

The arc-melted and vacuum arc-melted bulk alloys mostly achieve good cytocompatibility (Table 6), but they also show the strongest dependence on composition and post-treatment. TiZrHfNbTa, Sn-modified TiZrHfNbTa, TiNbTaZrMoV, and several TiZr-based refractory multi-principal-element alloys (RMPEAs) exhibited cytocompatibility comparable to that of Ti-6Al-4V. In addition, $Ti_{35}Zr_{35}Nb_{15}Mo_5Fe_5Cr_5$ alloy demonstrated that annealing improved cell viability and cell adhesion in comparison to as-cast condition [111]. Nevertheless, it should be mentioned that both conditions exceeded the ISO 10993-5 non-cytotoxic threshold, but the annealed condition gave higher live-cell density and more reviewed MG-63 cells than the as-cast state [111].

Table 6. The manufacturing methods, biocompatibility testing methods and key findings of the AM-ed Bio-HEAs

Alloys	Manufacturing method	Methods	Key findings	Reference
$Ti_{19.7}Zr_{19.6}Hf_{18.7}Nb_{19.8}Ta_{19.2}Sn_3$ $Ti_{19.2}Zr_{18.9}Hf_{18.8}Nb_{19.1}Ta_{19.1}Sn_{4.9}$ $Ti_{18.8}Zr_{18.4}Hf_{19.4}Nb_{18.2}Ta_{18.3}Sn_{6.9}$	arc-melting	MC3T3-E1 direct culture; live/dead microscopy	Non-cytotoxic and biocompatibility parallel to Ti-6Al-4V; viable-cell predominance reported for the Sn-containing HEAs	[101]
TiNbTaZrMo; TiNbTaZrMoV	vacuum arc-melting	Contact angle; CCK-8 days 1/3/5/7; SEM morphology; live/dead day 3	TiNbTaZrMoV contact angle 77.9±1.6°; no dead cells on live/dead staining; day-7 proliferation not significantly different from Ti-6Al-4V	[109]
316L-TiZrNbTa nanofilm; 316L-TiZrHfNbTa nanofilm	DC magnetron sputtering	Live/Dead; CCK-8; SEM; collagen secretion; Alizarin Red mineralization	RHEA nanofilm: E_{corr} −0.127 V; I_{corr} two orders lower than 316L substrate; osteoblast proliferative capacity ~1.5× substrate at day 5; best collagen secretion and ECM mineralization	[113]
TiZrNbTa HEA; TiZrNbTa-MONTs	MA & SPS	MC3T3-E1 proliferation assay; confocal/fluorescence morphology	Early proliferation lower on nanotubular surface at days 1 and 4, but day-7 OD reached 2.78 and was slightly above bare TiZrNbTa	[114]
TNZT; TNZT-hBN	SPS	MG-63 cytocompatibility testing; MTT/live-dead/adhesion imaging	hBN reinforcement did not impair biology; cell survival >95%, proliferation >95%, adhesion similar to unreinforced TNZT	[36]
MoTiZr; NbTiZr; MoTiVZr; NbTiVZr; NbMoTiZr	arc-melting	MC3T3-E1 CCK-8; crystal violet; cytoskeleton fluorescence	MoTiZr, NbTiZr, and NbMoTiZr showed cell shapes comparable to Ti-6Al-4V; V-containing MoTiVZr and NbTiVZr showed smaller, more elliptical cells	[112]
$Ti_{20}Zr_{20}Hf_{20}Nb_{20}Ta_{20}$	arc-melting	24 h SEM adhesion; 72 h live/dead; MTT over time; electrochemistry	No dead/unhealthy cells; no significant difference in adherent-cell density vs Ti-6Al-4V; corrosion rate on the order of 10^{-4} mm/year	[82]
$(MoTa)_xNbTiZr$ with selected $(MoTa)_{0.2}NbTiZr$ for biology	arc-melting	In vivo mouse thigh implantation; H&E histology; electrochemistry in PBS	Strong passive behavior in PBS; non-toxic soft-tissue response after 4 weeks in mice	[73]
TNZM1–TNZM4	cold-crucible levitation melting	$SaOS_2$ adhesion density and viability after 7 d	All four alloys showed good cytocompatibility; viability improved relative to empty-well control, with some composition dependence in adhesion density	[111]
$Ti_{35}Zr_{35}Nb_{15}Mo_5Fe_5Cr_5$ as-cast and annealed	vacuum arc melting	MTT at 3 and 7 d; AO/EtBr; SEM adhesion/morphology	Both conditions exceeded the ISO 10993-5 non-cytotoxic threshold; both surpassed 316L control viability, and annealed material showed more live cells and better adhesion than as-cast	[110]
ZrNbVTiAl	vacuum arc melting	U2OS attachment/growth; long-term exposure in biological medium	Substantial osteoblast attachment and growth; negligible bio-corrosion after 45 d; stronger attachment tendency than pure Ti	[51]
$Ti_{35}Zr_{15}Nb_{25}Mo_{15}Ta_{10}$ BIOHEA	vacuum arc melting	MG-63 adhesion imaging; MTT at 3/5/7 d; contact angle	Better wettability and better cell viability/proliferation than 316L stainless steel	[75]
MoNbTaTiZr	vacuum/argon arc melting	Stem-cell and osteoblast culture; morphology; tribo-corrosion-linked assessment	Stem cells and osteoblasts showed proliferation with filopodia indicating osteogenic commitment	[74]

SPS and mechanical alloying followed by SPS (MA-SPS) appear particularly promising when combined with surface modification (Table 6). SPS-processed TNZT-hBN maintained cell survival and proliferation above 95% despite hBN reinforcement, while MA-SPS TiZrNbTa showed improved biological performance after the formation of coral-like oxide nanotubes by anodization [36, 114]. DC magnetron sputtering also showed promising osteogenic performance, which was associated with the combined effects of nanofilm thickness, dense microstructure, post-annealing oxidation, and nanoscale surface morphology, resulting in improved corrosion resistance and osteoblast behavior (Table 6) [113].

5.2. Mechanistic interpretation and reported test metrics

The literature suggests a common pathway linking alloy processing to biological performance (Figure 5). Manufacturing and post treatment determine surface characteristics, including oxide chemistry, roughness, wettability, and topography, as well as corrosion and ion release behavior. Stable passive oxide films reduce ion release and minimize cytotoxicity risk, while favorable surface wettability and micro or nanoscale features promote protein adsorption and cell anchoring. These early interactions facilitate cell adhesion and spreading, leading to improved cell viability and proliferation. Under favorable conditions, this response can progress to enhanced osteogenic activity and extracellular matrix mineralization [82, 110, 113, 114].

The biological assessment methods used across the reviewed studies were consistent. MTT (3-(4,5-dimethylthiazol-2-yl)-2.5-diphenyltetrazolium bromide) was used in several studies and read at 570 nm, while CCK-8 was commonly read at 450 nm -> MTT was used in several studies, with absorbance measured at 570 nm, while CCK-8 was commonly measured at 450 nm.Live and dead assays used combinations such as calcein-AM/propidium iodide or AO/EtBr, and morphology was assessed by SEM, optical microscopy, confocal microscopy, or cytoskeletal fluorescence. Only a limited number of studies extended beyond basic cytocompatibility testing. For instance, Jia et al. added Direct Red 80 for collagen secretion and Alizarin Red for extracellular-matrix mineralization [113], while Akmal et al. used H&E histology after implantation [73]. Yadav et al. explicitly referenced ISO 10993-5, noting that relative viability above 70% indicates non-cytotoxicity [110].

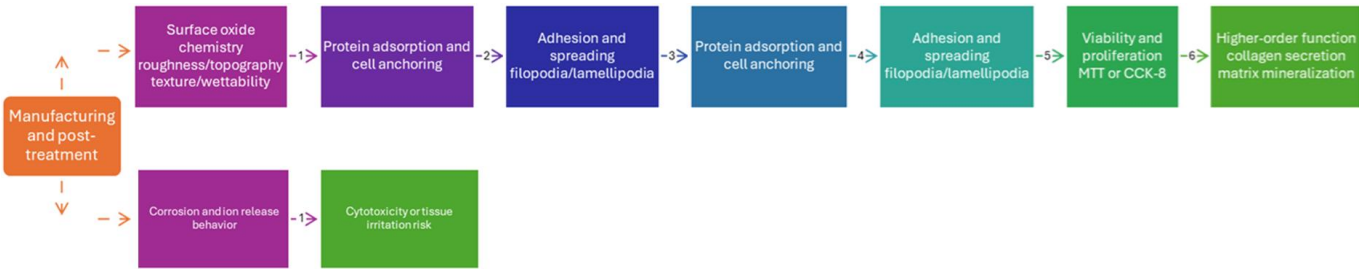


Figure 5. Schematic overview of the mechanisms by which manufacturing and post treatment affect surface characteristics, cell interactions, and biological performance of TiZrNbTa-containing high entropy alloys

Despite the generally positive findings, the available evidence remains limited. Most studies rely on short-term vitro assays using osteoblast or osteoblast-like cell lines, including MC3T3-E1, MG-63, SaOS2, and U2OS, with evaluation periods typically ranging from 24 h to 7 days. Furthermore, only one study reported in vivo implantation results, and only one extended the assessment to collagen secretion and extracellular matrix mineralization [73]. Therefore, while the current literature provides strong evidence for short-term cytocompatibility [36, 110, 111], it remains insufficient to fully evaluate long-term biological performance, immune compatibility, hemocompatibility, and osseointegration potential.

6. Future research

While significant progress has been made in the development of TiZrNbTa-based Bio-HEAs, several research gaps have still remained. Future developments should be focus on optimizing the composition of these alloys through a proper approach to controlling the concentrations of alloying elements, rather than relying solely on equiatomic designs. Specifically, it is essential to further investigate the effects of emerging alloying additions such as Zr, Mo, Hf, Sn, Fe, Si, and other biocompatible elements on phase stability, precipitation behavior, and mechanical performance.

From a processing perspective, direct comparisons of vacuum arc melting, powder metallurgy, SLM, electron beam powder bed fusion (EB-PBF), directed energy deposition (DED), spark plasma sintering (SPS), and post-processing techniques such as heat treatment, hot isostatic pressing (HIP), and severe plastic deformation should be conducted using identical alloy compositions. Conducting such studies will enhance understanding of how different manufacturing routes influence microstructural evaluation, phase formation, grain refinement, defects, and overall performance. Additionally, standardized characterization of grain structure, elemental segregation, oxide layer formation, porosity, and residual stress is needed to establish reliable processing–structure–property relationships. Also, needs to focus on Thermo-Calc calculations and lattice analysis to optimize the mechanical properties of TiZrNbTa-Bio HEAs.

Future research should move beyond basic cell viability assessments and focus on more comprehensive biological evaluation. Particular attention should be given to direct comparisons of different manufacturing routes using the same alloy composition, accompanied by standardized characterization of surface roughness, wettability, oxide chemistry, texture, and ion release behavior. Additional studies incorporating macrophage responses, co-culture systems, long-term osteogenic differentiation, and in vivo bone implantation models are also needed to better understand the clinical potential of these materials. Furthermore, combined investigations of wear, corrosion, and biological performance under physiological conditions would provide a more realistic assessment of implant behavior.

Based on the current evidence, the most promising approach is not solely the selection of TiZrNbTa based alloy compositions but the development of processing strategies that produce stable oxide films, high surface wettability, and favorable micro or nanoscale surface features capable of enhancing biological performance.

7. Conclusions

TiZrNbTa-based Bio-HEAs have emerged as one of the most promising classes of metallic biomaterials for next-generation implants. The studies reviewed indicate that these alloys predominantly exhibit stable body-centered cubic (BCC) solid-solution structures, which can be tailored through compositional modifications and processing optimization. Alloying additions such as Mo, Hf, Fe, Al, V, Ni and Ag significantly influence phase stability, microstructural evaluation, mechanical performance, corrosion resistance, and biological behavior.

Compared with conventional biomedical alloys, TiZrNbTa-based Bio-HEAs offer a unique combination of high strength, relatively low elastic modulus, excellent corrosion resistance, and favorable biocompatibility. The formation of stable passive oxide films rich in TiO_2, ZrO_2, Nb_2O_5, and Ta_2O_5 plays a critical role in enhancing corrosion resistance and reducing ion release in physiological environments. Furthermore, strategic alloying additions and advanced processing techniques provide effective approaches for optimizing the balance between strength, ductility, corrosion resistance, and biological performance. Although current studies demonstrate excellent short-term biocompatibility and promising mechanical and electrochemical properties, several challenges remain. In particular, long-term in vivo investigations and comprehensive clinical evaluations are still limited. In addition, the combined effects of alloy composition, processing route, surface modification, and biological response require further systematic investigation.

Future research should focus on the integrated optimization of composition, microstructure, processing methods, and surface engineering strategies to achieve superior long-term implant performance. Overall, TiZrNbTa-based Bio-HEAs represent a highly promising platform for the development of advanced biomedical implants with improved mechanical compatibility, corrosion resistance, and biocompatibility.

List of abbreviations

HEA	High entropy alloys
Bio-HEA	Bio High entropy alloys
VAM	Vacuum arc melting
PM	Powder metallurgy
AM	Additive manufacturing
BCC	Body-centered cubic
HCP	Hexagonal close-packed
FCC	Face-centered cubic
LMD	Laser metal deposition
TEM	Transmission electron microscopy
PCA	Process control agents
BEI	Back-scatter image
EBSD	Electron backscatter diffraction
XRD	X-ray Diffraction
KAM	Kernel average misorientation
HPT	High-pressure torsion
PBS	Phosphate buffer solution
FBS	Fetal bovine serum
SBF	Simulated body fluid
AO/EtBr	Acridine orange/ethidium bromide
Calcein-AM	Calcein acetoxymethyl ester
CCK-8	Cell counting kit-8
DC	Direct current
MC3T3-E1	Mouse calvaria-derived preosteoblastic cell line mc3t3-e1
MG-63	Human osteosarcoma cell line mg-63
MTT	3-(4.5-dimethylthiazol-2-yl)-2,5-diphenyltetrazolium bromide
OD	Optical density
RMPEAs	Refractory multi-principal element alloys
SaOS2	Human Osteosarcoma Cell Line saos-2
SPS	Spark plasma sintering
U2OS	Human osteosarcoma cell line u2os
XPS	X-ray Photoelectron Spectroscopy

Author contributions

Conceptualization: KNRS, AP; Data curation: KNRS, AZ; Formal analysis: KNRS, AZ; Funding acquisition: AP; Investigation: KNRS, AZ; Methodology: KNRS, AZ, AP; Project administration: AP; Resources: AP; Software: AP; Supervision: AP; Validation: AP; Visualization: KNRS, AZ; Writing – original draft: KNRS, AZ; Writing – review & editing: AP. All authors have read and agreed to the published version of the manuscript.

Funding

This research was funded by the Ministry of Science and Higher Education of the Republic of Kazakhstan under project No. AP26198929 «Design, Manufacturing & Characterization of Titanium based High Entropy Alloys lattices for Improved Mechanical, Electrochemical and Biological Behavior».

Acknowledgements

The authors express their sincere gratitude to the editor and anonymous reviewers for their constructive comments and valuable suggestions, which have significantly improved the quality of this manuscript.

Conflicts of interests

The authors declare no conflict of interest.

Data availability statement

The original contributions presented in this study are included in the article. Further inquiries can be directed to the corresponding author.

References

[1] Navarro, M., Michiardi, A., Castaño, O., & Planell, J. A. (2008). Biomaterials in orthopaedics. *Journal of The Royal Society Interface, 5(27)*, 1137-1158. https://doi.org/10.1098/rsif.2008.0151

[2] Saini, M., Yashpal, S., Pooja, A., Vipin, A., & Krati, J. (2015). Implant biomaterials: A comprehensive review. *World Journal of Clinical Cases, 3(1)*, 52. https://doi.org/10.12998/wjcc.v3.i1.52

[3] Zhu, D., Hu, S., Fu, Y., Zhao, N., & Liu, D. (2024). A review of preparation methods, friction and wear, corrosion, and biocompatibility of biomedical high-entropy alloys. *Journal of Materials Science, 59*(4), 1153-1183. https://doi.org/10.1007/s10853-023-09314-5

[4] Dawood, Z.H., Mohasien, A.M.N., & Hussein, S.K. (2026). Biocompatibility and mechanical properties of bio-high entropy alloys: A general review. *AIP Conf. Proc.* 3379, 060022. https://doi.org/10.1063/5.0306584

[5] Chen, Q., & Thouas, G. A. (2015). Metallic implant biomaterials. *Materials Science and Engineering R: Reports, 87*, 1-57. https://doi.org/10.1016/j.mser.2014.10.001

[6] Kaur, M., & Singh, K. (2019). Review on titanium and titanium-based alloys as biomaterials for orthopaedic applications. *Materials Science and Engineering C, 102*, 844-862. https://doi.org/10.1016/j.msec.2019.04.064

[7] Liu, C., Yang, C., Liu, J., Tang, Y., Lin, Z., Li, L., Liang, H., Lu, W., & Wang, L. (2022). Medical high-entropy alloy: Outstanding mechanical properties and superb biological compatibility. *Frontiers in Bioengineering and Biotechnology, 10*. https://doi.org/10.3389/fbioe.2022.952536

[8] Verran, J., & Whitehead, K. (2005). Factors affecting microbial adhesion to stainless steel and other materials used in medical devices. *International Journal of Artificial Organs, 28(11)*, 1138-1145. https://doi.org/10.1177/039139880502801111

[9] Ridzwan, M.I.Z., Shuib, S., Hassan, A.Y., Shokri, A.A., & Mohammad Ibrahim, M.N. (2007). Problem of stress shielding and improvement to the hip implant designs: A review. *Journal of Medical Sciences, 7*(3), 460-467. https://doi.org/10.3923/jms.2007.460.467

[10] Attarilar, S., Yang, J., Ebrahimi, M., Wang, Q., Liu, J., Tang, Y., & Yang, J. (2020). The Toxicity Phenomenon and the Related Occurrence in Metal and Metal Oxide Nanoparticles: A Brief Review from the Biomedical Perspective. *Frontiers in Bioengineering and Biotechnology, 8*. https://doi.org/10.3389/fbioe.2020.00822

[11] Choi-Yim, H., & Johnson, W.L. (1997). Bulk metallic glass matrix composites. *Applied Physics Letters, 71(26)*, 3808-3810. https://doi.org/10.1063/1.120512

[12] Peker, A., & Johnson, W.L. (1993). A highly processable metallic glass: Zr41.2Ti13.8Cu12.5Ni10.0Be22.5. *Applied Physics Letters, 63(17)*, 2342-2344. https://doi.org/10.1063/1.110520

[13] Yeh, J.W., Chen, S.K., Lin, S.J., Gan, J.Y., Chin, T.S., Shun, T.T., Tsau, C.H., & Chang, S.Y. (2004). Nanostructured high-entropy alloys with multiple principal elements: Novel alloy design concepts and outcomes. *Advanced Engineering Materials, 6(5)*, 299-303. https://doi.org/10.1002/adem.200300567

[14] Zhou, Y.J., Zhang, Y., Wang, Y.L., & Chen, G.L. (2007). Solid solution alloys of AlCoCrFeNi Tix with excellent room-temperature mechanical properties. *Applied Physics Letters, 90(18)*, 181904. https://doi.org/10.1063/1.2734517

[15] Edalati, P., Mohammadi, A., Ketabchi, M., & Edalati, K. (2021). Ultrahigh hardness in nanostructured dual-phase high-entropy alloy AlCrFeCoNiNb developed by high-pressure torsion. *Journal of Alloys and Compounds, 884*. https://doi.org/10.1016/j.jallcom.2021.161101

[16] Shuang, S., Yu, Q., Gao, X., He, Q. F., Zhang, J. Y., Shi, S. Q., & Yang, Y. (2022). Tuning the microstructure for superb corrosion resistance in eutectic high entropy alloy. *Journal of Materials Science and Technology, 109*, 197-208. https://doi.org/10.1016/j.jmst.2021.08.069

[17] Hori, T., Nagase, T., Todai, M., Matsugaki, A., & Nakano, T. (2019). Development of non-equiatomic Ti-Nb-Ta-Zr-Mo high-entropy alloys for metallic biomaterials. *Scripta Materialia, 172*, 83-87. https://doi.org/10.1016/j.scriptamat.2019.07.011

[18] Mohammed, M.T., Khan, Z.A., Geetha, M., Siddiquee, A.N., & Mishra, P. (2015). Influence of thermo-mechanical processing on microstructure, mechanical properties and corrosion behavior of a new metastable β-titanium biomedical alloy. *Bulletin of Materials Science, 38(1)*, 247-258. https://doi.org/10.1007/s12034-014-0832-5

[19] Wang, L., Xie, L., Lv, Y., Zhang, L. C., Chen, L., Meng, Q., Qu, J., Zhang, D., & Lu, W. (2017). Microstructure evolution and superelastic behavior in Ti-35Nb-2Ta-3Zr alloy processed by friction stir processing. *Acta Materialia, 131*, 499-510. https://doi.org/10.1016/j.actamat.2017.03.079

[20] Feng, J., Tang, Y., Liu, J., Zhang, P., Liu, C., & Wang, L. (2022). Bio-high entropy alloys: Progress, challenges, and opportunities. *Frontiers in Bioengineering and Biotechnology, 10*. https://doi.org/10.3389/fbioe.2022.977282

[21] Iki, M., Fujimori, K., Nakatoh, S., Tamaki, J., Ishii, S., Okimoto, N., Kamiya, K., & Ogawa, S. (2022). Delayed initiation of anti-osteoporosis medications increases subsequent hip and vertebral fractures in patients on long-term glucocorticoid therapy: A nationwide health insurance claims database study in Japan. *Bone, 160*, 116396. https://doi.org/10.1016/j.bone.2022.116396

[22] Mattia, L., Davis, S., Mark-Wagstaff, C., Abrahamsen, B., Peel, N., Eastell, R., & Schini, M. (2022). Utility of PINP to monitor osteoporosis treatment in primary care, the POSE study (PINP and Osteoporosis in Sheffield Evoluttion). *Bone, 158*, 116347. https://doi.org/10.1016/j.bone.2022.116347

[23] Aranda, V.A., Klyatskina, E., Barba-Pingarrón, A., Figueroa, I. A., Amigó, V., & Gonzalez, G. (2025). Nanoindentation and orientation imaging analysis of high entropy Ti–Nb–Zr–Ta–Mo alloys exhibiting dendrite microstructure. *Journal of Materials Research and Technology, 35*, 1732-1740. https://doi.org/10.1016/j.jmrt.2025.01.150

[24] Dobbelstein, H., Gurevich, EL., George, E.P., Ostendorf, A., & Laplanche, G. (2019). Laser metal deposition of compositionally graded TiZrNbTa refractory high-entropy alloys using elemental powder blends. *Additive Manufacturing, 25*, 252-262. https://doi.org/10.1016/j.addma.2018.10.042

[25] Xiang, T., Zhao, M., Du, P., & Xie, G. (2023). Heat treatment effects on microstructure and mechanical properties of TiZrNbTa high-entropy alloy. *Journal of Alloys and Compounds, 930*, 167408. https://doi.org/10.1016/j.jallcom.2022.167408

[26] Du, X., Ren, L., Wang, H., & Jian, W. (2026). Compositional evolution drives heterogeneity in NbTaTiVZr refractory multi-principal element alloys: Insights from experiment and phase-field simulation. *Applied Materials Today, 50*, 103184. https://doi.org/10.1016/j.apmt.2026.103184

[27] Li, Z., Lai, W., Tong, X., You, D., Li, W., & Wang, X. (2022). Design of TiZrNbTa multi-principal element alloys with outstanding mechanical properties and wear resistance. *Materials Science and Engineering: A, 845*, 143203. https://doi.org/10.1016/j.msea.2022.143203

[28] Qiao, Y., Tang, Y., Li, S., Ye, Y., Liu, X., Zhu, L., & Bai, S. (2020). Preparation of TiZrNbTa refractory high-entropy alloy powder by mechanical alloying with liquid process control agents. *Intermetallics, 126*, 106900. https://doi.org/10.1016/j.intermet.2020.106900

[29] González-Guillén, C., Romero-Resendiz, L., Naeem, M., Vidili, A.L., Otani, L.B., Klyatskina, E., Gonzalez, G., & Amigó, V. (2024). Microstructural and mechanical behavior of second-phase hardened porous refractory Ti-Nb-Zr-Ta alloys. *Journal of Alloys and Compounds, 980*, 173605. https://doi.org/10.1016/j.jallcom.2024.173605

[30] Lu, Y.S., Yamanaka, K., Bui, T.X., Hung, Y.X., Ishii, H., & Fang, T.H. (2025). Deformation mechanism of Nb(HfTa)xTiZr refractory high-entropy alloys. *International Journal of Mechanical Sciences, 307*, 110926. https://doi.org/10.1016/j.ijmecsci.2025.110926

[31] Liu, T.Y., Huang, J.C., Chuang, W.S., Chou, H.S., Wei, J.Y., Chao, C.Y., Liao, Y.C., & Jang, J.S.C. (2019). Spinodal decomposition and mechanical response of a TiZrNbTa high-entropy alloy. *Materials, 12*(21), 3508. https://doi.org/10.3390/ma12213508

[32] Namus, R.M., & Rainforth, W.M. (2024). Investigating the relevance of TiNbTaZr high entropy alloy for orthopaedic applications. *Wear, (548-549)*, 205393. https://doi.org/10.1016/j.wear.2024.205393

[33] Zhang, C., Wu, Y., You, L., Cao, X., Lu, Z., & Song, X. (2019). Investigation on the activation mechanism of hydrogen absorption in TiZrNbTa high entropy alloy. *Journal of Alloys and Compounds, 781*, 613-620. https://doi.org/10.1016/j.jallcom.2018.12.120

[34] Cao, P.P., Huang, H.L., Jiang, S.H., Liu, X.J., Wang, H., Wu, Y., & Lu, Z.P. (2022). Microstructural stability and aging behavior of refractory high entropy alloys at intermediate temperatures. *Journal of Materials Science and Technology, 122*, 243-254. https://doi.org/10.1016/j.jmst.2021.12.057

[35] Mustafi, L., Nguyen, V.T., Song, T., Deng, Q., Jiang, L., Chen, X.B., Fabijanic, D.M., & Qian, M. (2025). Effect of oxygen on the microstructure, tensile properties and deformation behaviours of a biocompatible Ti40Zr25Nb25Ta10 high entropy alloy. *Journal of Materials Science and Technology, 214*, 62-73. https://doi.org/10.1016/j.jmst.2024.06.022

[36] Digole, S., Garg, M., Bohara, S., Tsai, F.Y., Ahsan, S., Kothapalli, C.R., Gwalani, B., Young, D., Taheri, H., & Borkar, T. (2025). Microstructure evolution evolution, mechanical Properties, and biological Response of Ti-Nb-Zr-Ta (TNZT)/hBN metal matrix composites processed via spark plasma sintering (SPS). *Materials and Design, 260*, 115103. https://doi.org/10.1016/j.matdes.2025.115103

[37] Nguyen, V.T., Qian, M., Shi, Z., Tran, X Q., Fabijanic, D.M., Joseph, J., Qu, D.D., Matsumura, S., Zhang, C., Zhang, F., & Zou, J. (2020). Cuboid-like nanostructure strengthened equiatomic Ti–Zr–Nb–Ta medium entropy alloy. *Materials Science and Engineering: A, 798*, 140169. https://doi.org/10.1016/j.msea.2020.140169

[38] Zhang, X., Wang, W., Wu, J., Wang, S., Sun, J., Chung, J. Y., & Pennycook, S. J. (2021). Deformation twinning in Ti48.9Zr32.0Nb12.6Ta6.5 medium entropy alloy. *Materials Science and Engineering: A, 809*, 140931. https://doi.org/10.1016/j.msea.2021.140931

[39] Wang, B., Shan, X., Zhao, H., Bai, S., Wang, B., Tian, Y., & Tang, Y. (2023). High-temperature deformation behavior and microstructural evolution of NbZrTiTa refractory high entropy alloy. *Journal of Alloys and Compounds, 936*, 168059. https://doi.org/10.1016/j.jallcom.2022.168059

[40] Xiang, T., Cai, Z., Du, P., Li, K., Zhang, Z., & Xie, G. (2021). Dual phase equal-atomic NbTaTiZr high-entropy alloy with ultra-fine grain and excellent mechanical properties fabricated by spark plasma sintering. *Journal of Materials Science and Technology, 90*, 150-158. https://doi.org/10.1016/j.jmst.2021.03.024

[41] Roche, V., Champion, Y., Bataev, I.A., & Jorge Junior, A.M. (2022). Passive film formation on the new biocompatible non-equiatomicTi21Nb24Mo23Hf17Ta15 high entropy alloy before and after resting in simulated body fluid. *Corrosion Science, 207*, 110607. https://doi.org/10.1016/j.corsci.2022.110607

[42] Kasuga, T. (2019). Coatings for metallic biomaterials. *Metals for Biomedical Devices*, 369-382. https://doi.org/10.1016/B978-0-08-102666-3.00014-6

[43] Zhang, L.C., & Chen, L.Y. (2019). A Review on Biomedical Titanium Alloys: Recent Progress and Prospect. *Advanced Engineering Materials, 21(4)*, 1801215. https://doi.org/10.1002/adem.201801215

[44] Sidhu, S. S., Singh, H., & Gepreel, M. A. H. (2021). A review on alloy design, biological response, and strengthening of β-titanium alloys as biomaterials. *Materials Science and Engineering C, 121*, 111661. https://doi.org/10.1016/j.msec.2020.111661

[45] Kong, W., Cox, S.C., Lu, Y., Villapun, V., Xiao, X., Ma, W., Liu, M., & Attallah, M.M. (2021). The influence of zirconium content on the microstructure, mechanical properties, and biocompatibility of in-situ alloying Ti-Nb-Ta based β alloys processed by selective laser melting. *Materials Science and Engineering C, 131*, 112486. https://doi.org/10.1016/j.msec.2021.112486

[46] Solano-Orrala, D., Díaz-Cruces, E., Troconis, J., Zamora-Ledezma, E., Rodríguez-Díaz, J.M., Baltatu, M.S., Sandu, A.V., Hermoso-Gil, J., Alexis, F., Vizureanu, P., & Zamora-Ledezma, C. (2026). Advances in β-titanium alloys for safer and greener biomedical implants. *Biomaterials Advances, 183*, 214755. https://doi.org/10.1016/j.bioadv.2026.214755

[47] Wu, D., Isaksson, P., Ferguson, S. J., & Persson, C. (2018). Young's modulus of trabecular bone at the tissue level: *A review. In Acta Biomaterialia, 78*, 1-12. https://doi.org/10.1016/j.actbio.2018.08.001

[48] Uppal, G., Thakur, A., Chauhan, A., & Bala, S. (2022). Magnesium based implants for functional bone tissue regeneration – A review. *Journal of Magnesium and Alloys, 10(2)*, 356-386. https://doi.org/10.1016/j.jma.2021.08.017

[49] Moghadasi, K., Mohd Isa, M.S., Ariffin, M.A., Mohd jamil, M.Z., Raja, S., Wu, B., Yamani, M., Bin Muhamad, M.R., Yusof, F., Jamaludin, M.F., Ab Karim, M.S. bin, Abdul Razak, B. Binti, & Yusoff, N. Bin. (2022). A review on biomedical implant materials and the effect of friction stir based techniques on their mechanical and tribological properties. *Journal of Materials Research and Technology, 17*, 1054-1121. https://doi.org/10.1016/j.jmrt.2022.01.050

[50] Mustafi, L., Nguyen, V.T., Lu, S.L., Song, T., Murdoch, B.J., Fabijanic, D.M., & Qian, M. (2021). Microstructure, tensile properties and deformation behaviour of a promising bio-applicable new Ti35Zr15Nb25Ta25 medium entropy alloy (MEA). *Materials Science and Engineering: A, 824*, 141805. https://doi.org/10.1016/j.msea.2021.141805

[51] Chakraborty, P., Chittela, R.K., Samal, S., Sarkar, A., Rao, A.V. S.S.N., Neogy, S., & Tewari, R. (2024). Investigating the cyto-compatibility of ZrNbVTiAl high entropy alloy. *Journal of Alloys and Metallurgical Systems, 6*, 100076. https://doi.org/10.1016/j.jalmes.2024.100076

[52] Zollinger, J., & Fleury, E. (2020). Influence of Solidification Microstructure on Mechanical Properties of Al0.8CrCuFeNi2 High Entropy Alloy. *Frontiers in Materials, 7*. https://doi.org/10.3389/fmats.2020.00238

[53] Popescu, G., Ghiban, B., Popescu, C.A., Rosu, L., Truscă, R., Carcea, I., Soare, V., Dumitrescu, D., Constantin, I., Olaru, M. T., & Carlan, B. A. (2018). New TiZrNbTaFe high entropy alloy used for medical applications. IOP Conference Series: *Materials Science and Engineering, 400*, 022049. https://doi.org/10.1088/1757-899X/400/2/022049

[54] Li, Z., Lai, W., Tong, X., You, D., Li, W., & Wang, X. (2022). Design of TiZrNbTa multi-principal element alloys with outstanding mechanical properties and wear resistance. *Materials Science and Engineering: A, 845*, 143203. https://doi.org/10.1016/j.msea.2022.143203

[55] Li, W., Xie, D., Li, D., Zhang, Y., Gao, Y., & Liaw, P.K. (2021). Mechanical behavior of high-entropy alloys. *Progress in Materials Science, 118*, 100777. https://doi.org/10.1016/j.pmatsci.2021.100777

[56] Zhang, M., Zhou, X., & Li, J. (2017). Microstructure and Mechanical Properties of a Refractory CoCrMoNbTi High-Entropy Alloy. *Journal of Materials Engineering and Performance, 26(8)*, 3657-3665. https://doi.org/10.1007/s11665-017-2799-z

[57] Castro, D., Jaeger, P., Baptista, A.C., & Oliveira, J.P. (2021). An overview of high-entropy alloys as biomaterials. *Metals, 11(4)*, 648. https://doi.org/10.3390/met11040648

[58] Wang, R., Tang, Y., Ai, Y., Li, S., Zhu, L., & Bai, S. (2024). Strengthening and ductilization of a refractory high-entropy alloy over a wide strain rate range by multiple heterostructures. *International Journal of Plasticity, 173*, 103882. https://doi.org/10.1016/j.ijplas.2024.103882

[59] Sheikh, S., Shafeie, S., Hu, Q., Ahlström, J., Persson, C., Veselý, J., Zýka, J., Klement, U., & Guo, S. (2016). Alloy design for intrinsically ductile refractory high-entropy alloys. *Journal of Applied Physics, 120(16)*, 164902. https://doi.org/10.1063/1.4966659

[60] Todai, M., Nagase, T., Hori, T., Matsugaki, A., Sekita, A., & Nakano, T. (2017). Novel TiNbTaZrMo high-entropy alloys for metallic biomaterials. *Scripta Materialia, 129*, 65-68. https://doi.org/10.1016/j.scriptamat.2016.10.028

[61] Lei, N., Qin, J., Long, S., Zhang, C., Zhou, S., Yu, Z., & Yi, Y. (2026). Friction-corrosion behavior of (Ti42.5Zr42.5Nb10Ta5) 100- Mo (x = 0, 5) high-entropy alloys. *Tribology International, 219*, 111784. https://doi.org/10.1016/j.triboint.2026.111784

[62] Lin, M.Z, Xiao, X., Xu, C.H., Lu, W., Zhang, Y., & Liao, W.B. (2025). A nanostructured TiZrNbTaMo high-entropy alloy thin film with exceptional corrosion properties for biomedical application. *Applied Surface Science, 684*, 161859. https://doi.org/10.1016/j.apsusc.2024.161859

[63] Wu, P.S., Chao, H., Lin, S.J., Yang, Y.C., Hou, C. W., Lee, J. W., & Lou, B. S. (2024). Mechanical properties and biocompatibility evolution of TiZrNbTaFe high entropy alloy films deposited using a hybrid HiPIMS and RF sputtering system. *Surface and Coatings Technology, 494*, 131539. https://doi.org/10.1016/j.surfcoat.2024.131539

[64] Cantor, B., Chang, I.T.H., Knight, P., & Vincent, A.J.B. (2004). Microstructural development in equiatomic multicomponent alloys. *Materials Science and Engineering: A*, 375-377(1-2 SPEC. ISS.). https://doi.org/10.1016/j.msea.2003.10.257

[65] Wang, S.P., & Xu, J. (2017). TiZrNbTaMo high-entropy alloy designed for orthopedic implants: As-cast microstructure and mechanical properties. *Materials Science and Engineering C, 73*, 80-89. https://doi.org/10.1016/j.msec.2016.12.057

[66] Minciuna, M.G., Vizureanu, P., Geanta, V., Voiculescu, I., Sandu, A.V., Achitei, D.C., & Vitalariu, A.M. (2015). Effect of Si on the microstructure and mechanical properties of biomedical CoCrMo alloy. *Revista de Chimie*, *66*(6).

[67] Lei, N., Qin, J., Long, S., Zhang, C., Zhou, S., Yu, Z., & Yi, Y. (2026). Friction-corrosion behavior of (Ti42.5Zr42.5Nb10 Ta5)100- Mo (x = 0, 5) high-entropy alloys. *Tribology International*, *219*, 111784. https://doi.org/10.1016/j.triboint.2026.111784

[68] Qin, J., Yi, Y., Long, S., Ling, M., Zhong, L., Jin, F., Han, J., & Lai, W. (2024). Microstructure, mechanical properties and incipient plasticity of (Ti42.5Zr42.5Nb10Ta5)100-xMox refractory high-entropy alloys. *Journal of Materials Research and Technology*, *30*, 8128-8136. https://doi.org/10.1016/j.jmrt.2024.05.190

[69] Ishimoto, T., Ozasa, R., Nakano, K., Weinmann, M., Schnitter, C., Stenzel, M., Matsugaki, A., Nagase, T., Matsuzaka, T., Todai, M., Kim, H.S., & Nakano, T. (2021). Development of TiNbTaZrMo bio-high entropy alloy (BioHEA) super-solid solution by selective laser melting, and its improved mechanical property and biocompatibility. *Scripta Materialia*, *194*, 113658. https://doi.org/10.1016/j.scriptamat.2020.113658

[70] Wang, S.P., & Xu, J. (2018). (TiZrNbTa)-Mo high-entropy alloys: Dependence of microstructure and mechanical properties on Mo concentration and modeling of solid solution strengthening. *Intermetallics*, *95*, 59-72. https://doi.org/10.1016/j.intermet.2018.01.017

[71] Wang, S.P., & Xu, J. (2018). (TiZrNbTa)-Mo high-entropy alloys: Dependence of microstructure and mechanical properties on Mo concentration and modeling of solid solution strengthening. *Intermetallics*, *95*, 59-72. https://doi.org/10.1016/j.intermet.2018.01.017

[72] Shkodich, N.F., Kuskov, K.V., Sedegov, A.S., Kovalev, I.D., Panteleeva, A.V., Vergunova, Y.S., Scheck, Y.B., Panina, E., Stepanov, N., Serhiienko, I., & Moskovskikh, D. (2022). Refractory TaTiNb, TaTiNbZr, and TaTiNbZrX (X = Mo, W) high entropy alloys by combined use of high energy ball milling and spark plasma sintering: Structural characterization, mechanical properties, electrical resistivity, and thermal conductivity. *Journal of Alloys and Compounds*, *893*, 162030. https://doi.org/10.1016/j.jallcom.2021.162030

[73] Akmal, M., Hussain, A., Afzal, M., Lee, Y.I., & Ryu, H.J. (2021). Systematic Study of (MoTa)xNbTiZr Medium- and High-Entropy Alloys for Biomedical Implants- In Vivo Biocompatibility Examination. *Journal of Materials Science and Technology*, *78*, 183-191. https://doi.org/10.1016/j.jmst.2020.10.049

[74] Shittu, J., Pole, M., Cockerill, I., Sadeghilaridjani, M., Reddy, L. V. K., Manivasagam, G., Singh, H., Grewal, H. S., Arora, H. S., & Mukherjee, S. (2020). Biocompatible High Entropy Alloys with Excellent Degradation Resistance in a Simulated Physiological Environment. *ACS Applied Bio Materials*, *3(12)*, 8890-8900. https://doi.org/10.1021/acsabm.0c01181

[75] Rajabi, E., Dehghani, K., & Shahmir, H. (2026). Potential of TiZrNbMoTa high-entropy alloy for bone implant applications. *Next Bioengineering*, *2*, 100017. https://doi.org/10.1016/j.nxbio.2026.100017

[76] Li, H., Cai, Q., Li, S., & Xu, H. (2022). Effects of Mo equivalent on the phase constituent, microstructure and compressive mechanical properties of Ti–Nb–Mo–Ta alloys prepared by powder metallurgy. *Journal of Materials Research and Technology*, *16*, 588-598. https://doi.org/10.1016/j.jmrt.2021.12.054

[77] Wang, S., Wu, D., She, H., Wu, M., Shu, D., Dong, A., Lai, H., & Sun, B. (2020). Design of high-ductile medium entropy alloys for dental implants. *Materials Science and Engineering C*, *113*, 110959. https://doi.org/10.1016/j.msec.2020.110959

[78] An, Z., Mao, S., Liu, Y., Wang, L., Zhou, H., Gan, B., Zhang, Z., & Han, X. (2021). A novel HfNbTaTiV high-entropy alloy of superior mechanical properties designed on the principle of maximum lattice distortion. *Journal of Materials Science and Technology*, *79*, 109-117. https://doi.org/10.1016/j.jmst.2020.10.073

[79] Senkov, O.N., Scott, J.M., Senkova, S.V., Miracle, D.B., & Woodward, C.F. (2011). Microstructure and room temperature properties of a high-entropy TaNbHfZrTi alloy. *Journal of Alloys and Compounds*, *509(20)*, 6043-6048. https://doi.org/10.1016/j.jallcom.2011.02.171

[80] Juan, C.C., Tsai, M.H., Tsai, C.W., Hsu, W. L., Lin, C.M., Chen, S.K., Lin, S.J., & Yeh, J.W. (2016). Simultaneously increasing the strength and ductility of a refractory high-entropy alloy via grain refining. *Materials Letters*, *184*, 200-203. https://doi.org/10.1016/j.matlet.2016.08.060

[81] Gurel, S., Nazarahari, A., Canadinc, D., Cabuk, H., & Bal, B. (2021). Assessment of biocompatibility of novel TiTaHf-based high entropy alloys for utility in orthopedic implants. *Materials Chemistry and Physics*, *266*, 124573. https://doi.org/10.1016/j.matchemphys.2021.124573

[82] Yang, W., Liu, Y., Pang, S., Liaw, P. K., & Zhang, T. (2020). Bio-corrosion behavior and in vitro biocompatibility of equimolar TiZrHfNbTa high-entropy alloy. *Intermetallics*, *124*, 106845. https://doi.org/10.1016/j.intermet.2020.106845

[83] Berger, J.E., Jorge, A.M., Asato, G.H., & Roche, V. (2021). Formation of self-ordered oxide nanotubes layer on the equiatomic TiNbZrHfTa high entropy alloy and bioactivation procedure. *Journal of Alloys and Compounds*, *865*, 158837. https://doi.org/10.1016/j.jallcom.2021.158837

[84] Eleti, R.R., Stepanov, N., & Zherebtsov, S. (2020). Mechanical behavior and thermal activation analysis of HfNbTaTiZr body-centered cubic high-entropy alloy during tensile deformation at 77K. *Scripta Materialia*, *188*, 118-123. https://doi.org/10.1016/j.scriptamat.2020.07.028

[85] González-Masís, J., Cubero-Sesin, J. M., Campos-Quirós, A., & Edalati, K. (2021). Synthesis of biocompatible high-entropy alloy TiNbZrTaHf by high-pressure torsion. *Materials Science and Engineering: A*, *825*, 141869. https://doi.org/10.1016/j.msea.2021.141869

[86] Málek, J., Zýka, J., Lukáč, F., Vilémová, M., Vlasák, T., Čížek, J., Melikhova, O., Macháčková, A., & Kim, H.S. (2019). The effect of processing route on properties of HfNbTaTiZr high entropy alloy. *Materials*, *12(23)*, 4022. https://doi.org/10.3390/ma12234022

[87] Ding, J., Gao, J., Zhang, E., Tang, Y., Zhang, L., & Xia, X. (2025). Thermodynamic Modeling of the Ti-Hf-Zr-Nb-Ta Refractory High Entropy Alloy and Its Application in Analyzing Phase Stability. *Computers, Materials and Continua*, *85(1)*, 539-556. https://doi.org/10.32604/cmc.2025.067266

[88] Yuan, Y., Wu, Y., Yang, Z., Liang, X., Lei, Z., Huang, H., Wang, H., Liu, X., An, K., Wu, W., & Lu, Z. (2019). Formation, structure and properties of biocompatible TiZrHfNbTa high-entropy alloys. *Materials Research Letters*, *7(6)*, 225-231. https://doi.org/10.1080/21663831.2019.1584592

[89] Dobbelstein, H., Gurevich, E.L., George, E.P., Ostendorf, A., & Laplanche, G. (2018). Laser metal deposition of a refractory TiZrNbHfTa high-entropy alloy. *Additive Manufacturing*, *24*, 386-390. https://doi.org/10.1016/j.addma.2018.10.008

[90] Chen, Y., Fang, Y., Wang, R., Tang, Y., Bai, S., & Yu, Q. (2023). Achieving high strength and ductility in high-entropy alloys via spinodal decomposition-induced compositional heterogeneity. *Journal of Materials Science and Technology*, *141*, 149-154. https://doi.org/10.1016/j.jmst.2022.09.018

[91] Wang, W., Yang, K., Wang, Q., Dai, P., Fang, H., Wu, F., Guo, Q., Liaw, P. K., & Hua, N. (2022). Novel Ti-Zr-Hf-Nb-Fe refractory high-entropy alloys for potential biomedical applications. *Journal of Alloys and Compounds*, *906*, 164383. https://doi.org/10.1016/j.jallcom.2022.164383

[92] Ma, N., Liu, S., Liu, W., Xie, L., Wei, D., Wang, L., Li, L., Zhao, B., & Wang, Y. (2020). Research Progress of Titanium-Based High Entropy Alloy: Methods, Properties, and Applications. *Frontiers in Bioengineering and Biotechnology*, *8*. https://doi.org/10.3389/fbioe.2020.603522

[93] Cui, Y.W., Chen, L.Y., Qin, P., Li, R., Zang, Q., Peng, J., Zhang, L., Lu, S., Wang, L., & Zhang, L. C. (2022). Metastable pitting corrosion behavior of laser powder bed fusion produced Ti-6Al-4V in Hank's solution. *Corrosion Science*, *203*, 110333. https://doi.org/10.1016/j.corsci.2022.110333

[94] Khodaei, M., Nejatidanesh, F., Shirani, M. J., Iyengar, S., Sina, H., Valanezhad, A., & Savabi, O. (2020). Optimum temperature and chlorine ion concentration for hydrogen peroxide treatment

of titanium dental implant material. *Journal of Materials Research and Technology, 9(6),* 13312-13319. https://doi.org/10.1016/j.jmrt.2020.09.040

[95] Shi, Z., Fang, Q., Liaw, P.K., & Li, J. (2023). Corrosion-Resistant Biomedical High-Entropy Alloys: A Review. *Advanced Engineering Materials, 25(22),* 2300968. https://doi.org/10.1002/adem.202300968

[96] Guo, Z., Zhang, Z., Sun, Z., Qiang, Y., Shi, Y., Lv, X., & Shu, Q. (2025). Ta content-dependent phase evolution and corrosion resistance of ZrTiHfTax high-entropy alloys in 3-nitro-1,2,4-triazol-5-one (NTO) medium. *Defence Technology, 57,* 349-362. https://doi.org/10.1016/j.dt.2025.10.034

[97] Wang, H., Chen, W., Liu, S., Chu, C., Huang, L., Duan, J., Tian, Z., & Fu, Z. (2024). Exceptional combinations of tensile properties and corrosion resistance in a single-phase Ti1.6ZrNbMo0.35 refractory high-entropy alloy. *Intermetallics, 171,* 108349. https://doi.org/10.1016/j.intermet.2024.108349

[98] Niu, G., Yuan, R., Wang, E., Yang, X., Liu, Z., Li, Z., Zhang, Z., Gong, N., Li, K., Su, B., Zhang, J., Wu, H., Li, X., & Murr, L. E. (2024). Unraveling the influence of Mo on the corrosion mechanism of Ni-advanced weathering steel in harsh marine atmospheric environments. *Journal of Materials Science and Technology, 195,* 41-62. https://doi.org/10.1016/j.jmst.2024.02.021

[99] Guo, Y., Li, X., & Liu, Q. (2020). A novel biomedical high-entropy alloy and its laser-clad coating designed by a cluster-plus-glue-atom model. *Materials and Design, 196,* 109085. https://doi.org/10.1016/j.matdes.2020.109085

[100] Xu, Y.F., Xiao, Y.F., Yi, D.Q., Liu, H.Q., Wu, L., & Wen, J. (2015). Corrosion behavior of Ti-Nb-Ta-Zr-Fe alloy for biomedical applications in Ringer's solution. *Transactions of Nonferrous Metals Society of China, 25(8),* 2556-2563. https://doi.org/10.1016/S1003-6326(15)63875-4

[101] Yang, W., Pang, S.J., Wang, G., Liu, Y., Liaw, P.K., & Zhang, T. (2022). Ti–Zr–Hf–Nb–Ta–Sn high-entropy alloys with good properties as potential biomaterials. *Rare Metals, 41(7),* 2305-2315. https://doi.org/10.1007/s12598-021-01938-3

[102] Calin, M., Vishnu, J., Thirathipviwat, P., Popa, M. M., Krautz, M., Manivasagam, G., & Gebert, A. (2021). Tailoring biocompatible Ti-Zr-Nb-Hf-Si metallic glasses based on high-entropy alloys design approach. *Materials Science and Engineering C, 121,* 111733. https://doi.org/10.1016/j.msec.2020.111733

[103] Ma, F., Zhang, G., Liu, P., Chen, J., Liu, X., & Li, W. (2020). Effect of Various Annealing Temperature on Microstructure and Properties of Metastable β-Type Ti-35Nb-2Ta-3Zr Alloy for Biomedical Applications. *Frontiers in Materials, 7.* https://doi.org/10.3389/fmats.2020.00077

[104] Chui, P., Jing, R., Zhang, F., Li, J., & Feng, T. (2020). Mechanical properties and corrosion behavior of β-type Ti-Zr-Nb-Mo alloys for biomedical application. *Journal of Alloys and Compounds, 842,* 155693. https://doi.org/10.1016/j.jallcom.2020.155693

[105] Zhu, D., Li, X., Chai, S., Chee, T. S., Kim, C., Li, L., & Liu, D. (2025). evolution of wear, corrosion, and biocompatibility of a novel biomedical TiZr-based medium entropy alloy. *Journal of the Mechanical Behavior of Biomedical Materials, 165,* 106951. https://doi.org/10.1016/j.jmbbm.2025.106951

[106] Alamdari, A.A., Unal, U., & Motallebzadeh, A. (2022). Investigation of microstructure, mechanical properties, and biocorrosion behavior of Ti1.5ZrTa0.5Nb0.5W0.5 refractory high-entropy alloy film doped with Ag nanoparticles. *Surfaces and Interfaces, 28,* 101617. https://doi.org/10.1016/j.surfin.2021.101617

[107] Yang, W., Pang, S., Liu, Y., Wang, Q., Liaw, P.K., & Zhang, T. (2022). Design and properties of novel Ti–Zr–Hf–Nb–Ta high-entropy alloys for biomedical applications. *Intermetallics, 141,* 107421. https://doi.org/10.1016/j.intermet.2021.107421

[108] Hussein, M.A., Abdul Azeem, M., Kumar, A.M., & Ankah, N. (2025). Design and Development of Ti–Zr–Nb–Ta–Ag High Entropy Alloy for Bioimplant Applications. *Advanced Engineering Materials, 27(6),* 2400462. https://doi.org/10.1002/adem.202400462

[109] Lai, K.C., Chao, S.C., Tseng, K.K., Yeh, J.W., & Chen, P.Y. (2023). Biocompatible as-cast and homogenized TiNbTaZrMoV high entropy alloys: mechanical properties, corrosion resistance and in vitro studies. *Journal of Materials Research and Technology, 24,* 9708-9721. https://doi.org/10.1016/j.jmrt.2023.05.201

[110] Yadav, D.K., Paliwal, D., Yadav, S.D., & Sinha, S. (2026). Crystallographic texture dependence of biocompatibility in a Ti35Zr35Nb15Mo5Fe5Cr5 complex concentrated alloy. *Materialia, 45,* 102623. https://doi.org/10.1016/j.mtla.2025.102623

[111] Weng, W., Biesiekierski, A., Lin, J., Ozan, S., Li, Y., & Wen, C. (2021). Development of beta-type Ti-Nb-Zr-Mo alloys for orthopedic applications. *Applied Materials Today, 22,* 100968. https://doi.org/10.1016/j.apmt.2021.100968

[112] Gong, J., Liu, J., Song, X., Li, Y., Wang, Y., & Chen, Z. (2024). Investigations on microstructure and properties of five TiZr-based refractory multi-principal element alloys for clinical metallic biomaterials. *Journal of Alloys and Compounds, 995,* 174823. https://doi.org/10.1016/j.jallcom.2024.174823

[113] Jia, W., Gong, Y., Zheng, K., Ma, Y., Zheng, X., Wu, Y., Zhou, B., Gao, J., & Yu, S. (2024). Mechanical properties and biological behavior of refractory TiZrNbTa medium-entropy and TiZrHfNbTa high-entropy alloy nanofilms on AISI 316L for bone implants. *Materials Characterization, 216,* 114253. https://doi.org/10.1016/j.matchar.2024.114253

[114] Xiang, T., Bao, W., Zhao, M., Du, P., Cai, Z., & Xie, G. (2022). Ultra-high strength TiZrNbTa high entropy alloy substrate coated by coral-like metal oxide nanotubes to enhance biocompatibility. *Journal of Alloys and Compounds, 923,* 166408. https://doi.org/10.1016/j.jallcom.2022.166408

Ti–Zr–Nb–Ta негізіндегі биомедициналық қолдануға арналған био-жоғары энтропиялық қорытпаларға шолу

Х.Н.Р. Шайк, А. Жумабекова, А. Первин*

Инженерия мектебі, Назарбаев Университеті, Астана, Қазақстан

**Корреспонденция үшін автор: asma.perveen@nu.edu.kz*

Аңдатпа. Заманауи биомедициналық имплантаттарға деген сұраныстың артуы механикалық үйлесімділігі, коррозияға төзімділігі және биосәйкестілігі жоғары жаңа металл биоматериалдарды әзірлеуге ықпал етті. Ti–6Al–4V, Co–Cr–Mo қорытпалары және тот баспайтын болат сияқты дәстүрлі имплантат материалдарының кернеуді экрандау әсері, иондардың бөлінуі және ұзақ мерзімді биологиялық қауіпсіздікке қатысты мәселелер сияқты бірқатар кемшіліктері бар. Осыған байланысты TiZrNbTa негізіндегі био-жоғары энтропиялық қорытпалар (био-ЖЭҚ) құрамында биосәйкесті элементтердің болуы, жоғары беріктігі, төмен серпімділік модулі, жоғары коррозияға төзімділігі және жақсы биосәйкестілігі арқасында болашағы зор биоматериалдар ретінде қарастырылуда. Бұл шолуда TiZrNbTa негізіндегі био-ЖЭҚ бойынша соңғы ғылыми жетістіктер жинақталып, олардың микроқұрылымы, легірлеу стратегиялары, меха-

никалық қасиеттері, коррозиялық қасиеттері және биосәйкестілігі қарастырылды. Талдауға алынған зерттеулер TiZrNbTa негізіндегі био-ЖЭҚ-тың тұрақты көлемдік-центрленген кубтық (КЦК) қатты ерітінді құрылымына ие екенін көрсетті. Сонымен қатар, олардың фазалық тұрақтылығы мен микроқұрылымдық ерекшеліктері химиялық құрамды өзгерту, термомеханикалық өңдеу және заманауи өндіру технологияларын қолдану арқылы реттелуі мүмкін. Құрамы мен өңдеу жағдайларына байланысты TiZrNbTa негізіндегі био-ЖЭҚ-тың серпімділік модулі 57-135 ГПа аралығында, ал аққыштық шегі 1000 МПа-дан жоғары болып, механикалық беріктік пен адам сүйек тінімен үйлесімділіктің оңтайлы үйлесімін қамтамасыз етеді. Сонымен қатар, TiO_2, ZrO_2, Nb_2O_5 және Ta_2O_5 оксидтеріне бай тұрақты пассивті оксидті қабықшалардың түзілуі физиологиялық ортада жоғары коррозияға төзімділікті қамтамасыз етеді. Биосәйкестілік бойынша жүргізілген зерттеулер қолайлы биологиялық жауаптарды көрсетіп, TiZrNbTa негізіндегі био-ЖЭҚ-тың ортопедиялық және стоматологиялық имплантаттарда қолдануға жоғары әлеуетке ие екенін дәлелдеді. Соңында жаңа буын биомедициналық имплантаттарын әзірлеуге қатысты негізгі мәселелер мен болашақ зерттеу бағыттары қарастырылды.

Негізгі сөздер: *био-жоғары энтропиялық қорытпалар, TiZrNbTa, микроқұрылым, механикалық қасиеттер, биосәйкестілік, легірлеуші элементтер.*

Биосовместимые высокоэнтропийные сплавы на основе системы Ti-Zr-Nb-Ta для биомедицинского применения: всесторонний обзор

Х.Н.Р. Шайк, А. Жумабекова, А. Первин*

Школа инженерии, Назарбаев Университет, Астана, Казахстан

**Автор для корреспонденции: asma.perveen@nu.edu.kz*

Аннотация. Растущая потребность в современных биомедицинских имплантатах стимулирует разработку новых металлических биоматериалов с улучшенной механической совместимостью, коррозионной стойкостью и биосовместимостью. Традиционные материалы для имплантатов, такие как Ti–6Al–4V, сплавы Co–Cr–Mo и нержавеющая сталь, часто имеют ряд ограничений, включая эффект экранирования напряжений, высвобождение ионов и проблемы, связанные с долгосрочной биологической безопасностью. Среди новых биоматериалов био-высокоэнтропийные сплавы (био-ВЭС) на основе TiZrNbTa рассматриваются как перспективные материалы благодаря сочетанию биосовместимых элементов, высокой прочности, низкого модуля упругости, высокой коррозионной стойкости и благоприятной биосовместимости. В данном обзоре представлены современные достижения в области био-ВЭС на основе TiZrNbTa с особым акцентом на оценку микроструктуры, стратегии легирования, механические свойства, коррозионное поведение и биосовместимость. Проанализированные исследования показывают, что био-ВЭС на основе TiZrNbTa характеризуются стабильной однофазной твердорастворной структурой с объемно-центрированной кубической (ОЦК) кристаллической решеткой. При этом фазовая стабильность и микроструктурные характеристики могут регулироваться путем изменения химического состава, термомеханической обработки и применения современных технологий изготовления. В зависимости от состава и условий обработки модуль упругости био-ВЭС на основе TiZrNbTa составляет от 57 до 135 ГПа, а предел текучести превышает 1000 МПа, обеспечивая благоприятное сочетание высокой механической прочности и совместимости с костной тканью человека. Кроме того, образование стабильных пассивных оксидных пленок, обогащенных TiO_2, ZrO_2, Nb_2O_5 и Ta_2O_5, обеспечивает высокую коррозионную стойкость в физиологических средах. Исследования биосовместимости продемонстрировали благоприятный биологический отклик, что подтверждает высокий потенциал био-ВЭС на основе TiZrNbTa для применения в ортопедических и стоматологических имплантатах. В заключение рассмотрены существующие проблемы и перспективные направления дальнейших исследований, направленных на разработку биомедицинских имплантатов нового поколения.

Ключевые слова: *био-высокоэнтропийные сплавы, TiZrNbTa, микроструктура, механические свойства, биосовместимость, легирующие элементы.*

Publisher's note

All claims expressed in this manuscript are solely those of the authors and do not necessarily represent those of their affiliated organizations, or those of the publisher, the editors and the reviewers.